Spin-orbit coupling from a two-component self-consistent approach. II. Non-collinear density functional theories

Spin-Orbit Coupling from a Two-Component Self-Consistent Approach. Part II: Non-Collinear Density Functional Theories

Jacques K. Desmarais,[1,2,3,a] Jean-Pierre Flament,[4] and Alessandro Erba[1,b]
[1] *Dipartimento di Chimica, Università di Torino, Via Giuria 5, 10125 Torino, Italy*
[2] *Department of Geological Sciences, University of Saskatchewan, Saskatoon, SK S7N 5E2, Canada*
[3] *Department of Physics and Engineering Physics, University of Saskatchewan, Saskatoon, SK S7N 5E2, Canada*
[4] *Laboratoire de Physique des Lasers et des Molecules, UFR de Physique, Batiment P5, Universite de Lille, 59655 Villeneuve D'Ascq Cedex, France*

(Dated: 23 July 2019)

We revise formal and numerical aspects of collinear and non-collinear density functional theory (DFT) in the context of a two-component self-consistent treatment of spin-orbit coupling (SOC). While the extension of the standard one-component theory to a non-collinear magnetization is formally well-defined within the local density approximation (LDA), and therefore results in a numerically stable theory, this is not the case within the generalized gradient approximation (GGA). Previously reported formulations of non-collinear DFT based on GGA exchange-correlation potentials have several limitations: i) they fail at reducing (either formally or numerically) to the proper collinear limit (i.e. when the magnetization is parallel to the z axis everywhere in space); ii) they fail at ensuring a quantitative rotational invariance of the total energy and even a qualitative rotational invariance of the spatial distribution of the magnetization when a SOC operator is included in the Hamiltonian; iii) they are numerically very unstable in regions of small magnetization. All of the above mentioned problems are here shown (both formally and through test examples) to be solved by using instead a new formulation of non-collinear DFT for GGA functionals, which we call the "signed canonical" theory, as combined with an effective screening algorithm for unstable terms of the exchange-correlation potential in regions of small magnetization. All methods are implemented in the CRYSTAL program and tests are performed on simple molecules to compare the different formulations of non-collinear DFT.

Keywords: non-collinear DFT, relativistic DFT, spin-orbit coupling, collinear limit, rotational invariance

I. INTRODUCTION

There is great interest in the generalization of the density functional theory (DFT) to non-collinear (NC) spin densities and spin-orbit coupling (SOC). This is in part because, nowadays, the DFT is the method of choice for studying extended systems from a first principles approach. A NC formulation of the DFT is necessary for treating SOC because rotational invariance is otherwise lost in the usual collinear theory, when a SOC operator is included in the Hamiltonian. While in principle a well-defined strategy for the formal derivation of relativistic DFT has been formulated – based either on the relativistic four-current density in the four-component case or on the electron density, magnetization and orbital current-density in the two-component case – in practice, there is a lack of any density functional approximations (DFAs) built using such a theory.[1–4] As a consequence, practical implementations of relativistic NC-DFT usually need to be formulated in a manner much closer to its non-relativistic counterpart.[5–16] In this respect, one exception is represented by the use of such formal definition of relativistic two-component DFT as combined with the so-called optimized effective potential method, where the exact exchange functional is adopted. However, this approach turns out to be very similar to the Hartree-Fock (HF) theory, and provides essentially no advantages over the latter (apart from leading to a local versus non-local potential), as it also lacks any treatment of electron correlation.[17,18]

Wavefunction-based methods can be generalized in a well-defined and formally straightforward way to NC spin densities and spin-orbit coupling. For instance, this is the case for the spin-orbit configuration-interaction (SO-CI) approach[19,20] and the two- or four-component coupled-cluster (SO-CCSD) approach.[21] However, such approaches are often not applicable to extended systems, either because they are too expensive (like in the case of SO-CCSD) or because they are not size-extensive (like in the case of SO-CI). This further exacerbates the need for efficient generalizations of the DFT to NC magnetism and SOC.

The most common method to generalize the DFT to NC magnetism and SOC is the approach first described by Kubler and co-workers, originally formulated for the local-density approximation (LDA) and hereafter referred to as the "canonical" non-collinear theory.[5] At variance with the usual non-relativistic collinear theory (where the spin-quantisation axis is taken everywhere along z), the quantisation axis is now allowed to vary

[a] Electronic mail: jkd788@mail.usask.ca
[b] Electronic mail: alessandro.erba@unito.it

from point to point and to locally adopt the direction of the electron magnetization. When used with LDA functionals, the theory is numerically very stable and also reduces properly to the result of the corresponding collinear functional when the magnetization is indeed parallel everywhere (the so-called "collinear limit"). Considerable work has also gone towards implementing this formulation for time-dependent DFT.[22–28] Several attempts have been made to generalize this canonical non-collinear theory to functionals beyond the simple LDA.[7,8,10–12,29,30] In all cases, serious numerical problems have been reported. Sometimes, these problems have been partly circumvented by throwing away unstable terms in the exchange-correlation (xc) potential.[10–12] However, such a prescription is to be considered undesirable as, among other reasons, it can lead to inaccuracies and non-variational energies, which can hamper subsequent calculations of energy derivatives. In other cases, the actual approach used beyond LDA is not entirely outlined,[8] or the numerical instability of the implementation is acknowledged in later publications.[6,7] Moreover, there are also some formal problems with the canonical theory, which make straightforward generalizations to generalized-gradient (GGA) or meta-GGA functionals to no longer reduce to the proper collinear limit. This has been previously acknowledged by Scalmani and Frisch.[9] As a result, generalizations of the canonical NC theory to functionals beyond the LDA is seldom used in applications.

In order to circumvent these numerical and formal problems, Scalmani and Frisch (SF) have recently proposed an alternative formulation of NC-DFT, originally used in the absence of SOC, for functionals beyond the LDA (GGAs and meta-GGAs).[9] However, we show for GGAs that while the SF xc functional reduces to the proper collinear limit, the SF xc potential does not.

Motivated by these shortcomings, in this study we present a new formulation of NC-DFT to be used with and without SOC, which we call the "signed canonical" non-collinear theory. The enhanced stability, rotational invariance and reduction to the proper collinear limit are shown first through a comparative formal analysis against the previously proposed theories, and then through explicit test examples on some small molecular systems. Our suggested procedure is a modification of the canonical non-collinear formulation, but in principle it could also be used to modify the SF formulation. Our NC-DFT theory will be shown in the following to be especially promising in conjunction with the generalized HF procedure outlined in Part I for calculations with hybrid functionals.[31] All the formulations of NC-DFT discussed in the paper have been implemented in a developmental version of the public CRYSTAL program.[32]

II. FORMAL ASPECTS

We refer to Part I of the paper for the description of the adopted notation, in particular for a description of the adopted notation for vectors and matrices.[31] The present implementation is based on a two-component Kramers-unrestricted approach, where spin-orbit coupling (SOC), as well as scalar-relativistic (SR), effects are both treated self-consistently from relativistic effective-core potential (RECP) operators. These are mono-electronic, non-local operators which enter into the Hamiltonian and are obtained by fitting a set of solid-spherical Gaussian functions to potentials derived from comparatively very accurate all-electron four-component atomic Dirac-Fock calculations.[33,34]

The presence of the SOC operator implies that the eigenfunctions of the Hamiltonian are complex two-component spinors, which, in our case, are in turn expanded as a linear combination of n_f real-atomic orbitals $\chi_\mu(\underline{\mathbf{r}})$:

$$\mathbf{\Psi}_i(\underline{\mathbf{r}}) = \sum_{\mu=1}^{n_f} \left[\begin{pmatrix} c^{\alpha}_{\mu,i} \\ 0 \end{pmatrix} + \begin{pmatrix} 0 \\ c^{\beta}_{\mu,i} \end{pmatrix} \right] \chi_\mu(\underline{\mathbf{r}}) \; , \qquad (1)$$

where $c^{\sigma}_{\mu,i}$ (with $\sigma = \alpha, \beta$) are complex molecular orbital (MO) coefficients that are determined by solving the corresponding self-consistent field (SCF) equations (either Fock or Kohn-Sham). From the subset of occupied two-component MO spinors in Eq. (1), a complex-Hermitian one-particle density matrix is built as:

$$\left[D^{\sigma\sigma'}\right]_{\mu\nu} \equiv \sum_{i}^{occ} \left[c^{\sigma}_{\mu i}\right]^{*} c^{\sigma'}_{\nu i} \; . \qquad (2)$$

In the present implementation in the CRYSTAL code, the χ_μ atomic orbitals are expressed as a linear combination of real solid-spherical Gaussian-type functions up to angular momentum quantum number $l = 4$ (i.e. g-type functions).[35]

A. Fundamental Variables in Relativistic Density Functional Theory

Any practical formulation of the density functional theory requires a definition of fundamental variables (i.e. basic ingredients) from which density functional approximations (DFAs) are built. Although the most general formulation of relativistic DFT would be based on the four-current (i.e. the generalization of the electron density within a four-component relativistic treatment), in practice no DFAs are built from it so that relativistic exchange-correlation functionals are typically defined in terms of variables more closely related to their non-relativistic counterparts.[2]

As is now common-practice for most calculations on systems bigger than one atom,[2,5–14,36] here we consider

DFAs based on the particle-number (or total) density:

$$n(\underline{\mathbf{r}}) \equiv \sum_{i}^{occ} \mathbf{\Psi}_i^\dagger(\underline{\mathbf{r}})\mathbf{\Psi}_i(\underline{\mathbf{r}}) \; , \tag{3}$$

and on the magnetization vector $\underline{\mathbf{m}}(\underline{\mathbf{r}})$, whose Cartesian components are defined as:

$$m_c(\underline{\mathbf{r}}) \equiv \sum_{i}^{occ} \mathbf{\Psi}_i^\dagger(\underline{\mathbf{r}})\hat{\boldsymbol{\sigma}}_c\mathbf{\Psi}_i(\underline{\mathbf{r}}) \; , \tag{4}$$

where $c = x, y, z$ labels a Cartesian component and $\hat{\boldsymbol{\sigma}}_c$ are the usual 2×2 complex Pauli matrices given in Eq. (4) of Part I. By introducing the following compact notation:

$$\begin{aligned} n^{\Re}_{\sigma\sigma'}(\underline{\mathbf{r}}) &= \sum_{\mu\nu} \Re\Big[D^{\sigma\sigma'}\Big]_{\mu\nu}\chi_\mu(\underline{\mathbf{r}})\chi_\nu(\underline{\mathbf{r}}) \; ; \\ n^{\Im}_{\sigma\sigma'}(\underline{\mathbf{r}}) &= \sum_{\mu\nu} \Im\Big[D^{\sigma\sigma'}\Big]_{\mu\nu}\chi_\mu(\underline{\mathbf{r}})\chi_\nu(\underline{\mathbf{r}}) \; , \end{aligned} \tag{5}$$

the total density and magnetization can be expressed in terms of the elements of the density matrix as follows:[31]

$$n(\underline{\mathbf{r}}) = n^{\Re}_{\alpha\alpha}(\underline{\mathbf{r}}) + n^{\Re}_{\beta\beta}(\underline{\mathbf{r}}) \; ; \tag{6}$$

$$m_x(\underline{\mathbf{r}}) = n^{\Re}_{\alpha\beta}(\underline{\mathbf{r}}) + n^{\Re}_{\beta\alpha}(\underline{\mathbf{r}}) \; ; \tag{7}$$

$$m_y(\underline{\mathbf{r}}) = n^{\Im}_{\alpha\beta}(\underline{\mathbf{r}}) - n^{\Im}_{\beta\alpha}(\underline{\mathbf{r}}) \; ; \tag{8}$$

$$m_z(\underline{\mathbf{r}}) = n^{\Re}_{\alpha\alpha}(\underline{\mathbf{r}}) - n^{\Re}_{\beta\beta}(\underline{\mathbf{r}}) \; . \tag{9}$$

The common restriction to DFAs built solely from n and $\underline{\mathbf{m}}$ introduced above represents a limitation in the context of two-component relativistic DFT as it neglects contributions from the so-called "orbital current-density".[3,37] Nonetheless, let us note here that, interestingly, the physics contained in the orbital current-density can be recovered into the two-component DFT description by using so-called hybrid exchange-correlation functionals, where a fraction of non-local exact Fock exchange is included.[37]

B. Generalized DFT Treatment

We now discuss the treatment of SOC within the DFT in a two-component framework. Here we show how the approach can be generalized to local-density and generalized-gradient approximations (LDA and GGA) of the exchange-correlation (xc) operator, as well as LDA and GGA hybrid functionals, where a fraction a of non-local Fock exchange is included in its definition. That is to say, we are interested in formulations of DFT associated with energy expressions of the form:

$$E = \mathrm{Tr}\left(\mathbf{h}\mathbf{D}^\dagger\right) + \frac{1}{2}\mathrm{Tr}\left(\mathbf{C}\mathbf{D}^\dagger\right) + \frac{a}{2}\mathrm{Tr}\left(\mathbf{K}\mathbf{D}^\dagger\right) + E_{xc}[\underline{\mathbf{Q}}] \tag{10}$$

The exact form of the mono-electronic $\mathbf{h}$ matrix elements, and bi-electronic Coulomb $\mathbf{C}$ and exchange $\mathbf{K}$ matrix elements, as well as strategies for calculating the traces above were discussed in Part I.[31] The formal analyses presented here depend on the formulation of the xc approximation (i.e. whether the functional is of LDA or GGA type), but not on the specific form of the functional itself. E_{xc} is the exchange-correlation energy, which is expressed using integrals over space of the exchange-correlation functional F_{xc}:

$$E_{xc} = (1-a)\int F_x[\underline{\mathbf{Q}}]d\underline{\mathbf{r}} \; + \; \int F_{\mathrm{corr}}[\underline{\mathbf{Q}}]d\underline{\mathbf{r}} \; , \tag{11}$$

where the exchange-correlation functional has been written as a sum of exchange F_x and correlation F_{corr} contributions:

$$F_{xc}[\underline{\mathbf{Q}}] \equiv F_x[\underline{\mathbf{Q}}] + F_{\mathrm{corr}}[\underline{\mathbf{Q}}] \; . \tag{12}$$

For $a = 0$, the formalism reduces to that of plain LDA or GGA formulations. In the above, the exchange-correlation functional depends on a set of variables $\underline{\mathbf{Q}}$. More explicitly, $\underline{\mathbf{Q}}$ is spanned by density variables $n_\pm$ and gradient variables $\gamma_{\pm\pm}$:

$$\underline{\mathbf{Q}}(\underline{\mathbf{r}}) = [n_+(\underline{\mathbf{r}}), n_-(\underline{\mathbf{r}}), \gamma_{++}(\underline{\mathbf{r}}), \gamma_{--}(\underline{\mathbf{r}}), \gamma_{+-}(\underline{\mathbf{r}})] \; . \tag{13}$$

The density variables $n_\pm$ depend on the value of the total density and magnetization at position $\underline{\mathbf{r}}$ in space, while the gradient variables $\gamma_{\pm\pm}$ depend on both the value and gradients (with respect to $\underline{\mathbf{r}}$) of the total density and magnetization at position $\underline{\mathbf{r}}$ in space. So the variables $\gamma_{\pm\pm}$ are proper to GGA functionals, whereas the $n_\pm$ are present in both LDA and GGA functionals. More details on the exact definitions of these variables are provided in the following. In principle, meta-GGA forms of the exchange-correlation operator could also be treated similarly using however a larger set of variables, but we do not discuss these explicitly here.

The Kohn-Sham Hamiltonian is built using the xc potential $\hat{\mathbf{V}}_{xc}$, which is also written as a sum of exchange and correlation contributions:

$$\hat{\mathbf{V}}_{xc}(\underline{\mathbf{r}}) \equiv \hat{\mathbf{V}}_x(\underline{\mathbf{r}}) + \hat{\mathbf{V}}_{\mathrm{corr}}(\underline{\mathbf{r}}) \; , \tag{14}$$

and, within a two-component generalisation of the theory, is given by:[5,7,38]

$$\hat{\mathbf{V}}_{xc}(\underline{\mathbf{r}}) = \mathcal{E}^{xc}(\underline{\mathbf{r}})\hat{\boldsymbol{\sigma}}_0 + \sum_c \mathcal{B}_c^{xc}(\underline{\mathbf{r}})\hat{\boldsymbol{\sigma}}_c \; , \tag{15}$$

where the $\hat{\boldsymbol{\sigma}}_c$ are the 2×2 complex Pauli matrices, $\hat{\boldsymbol{\sigma}}_0$ is the 2×2 identity matrix, and both $\mathcal{E}^{xc}$ and $\mathcal{B}_c^{xc}$ are defined in terms of functional derivatives of the xc energy. More specifically, the xc electrostatic potential $\mathcal{E}^{xc}$ reads:

$$\mathcal{E}^{xc}(\underline{\mathbf{r}}) = \frac{\delta E_{xc}}{\delta n_+(\underline{\mathbf{r}})} + \frac{\delta E_{xc}}{\delta n_-(\underline{\mathbf{r}})} \; , \tag{16}$$

and the Cartesian components $\mathcal{B}_c^{xc}$ of the so-called xc magnetic field read:

$$\mathcal{B}_c^{xc}(\underline{\mathbf{r}}) = \frac{m_c(\underline{\mathbf{r}})}{m(\underline{\mathbf{r}})}\left[\frac{\delta E_{xc}}{\delta n_+(\underline{\mathbf{r}})} - \frac{\delta E_{xc}}{\delta n_-(\underline{\mathbf{r}})}\right] \; , \tag{17}$$

where $m \equiv |\underline{\mathbf{m}}|$ (in the NC theory, see below) or $m \equiv m_z$ (in the collinear theory) and, in the expressions above, δ is used to represent the functional derivative.

We can use the $\underline{\boldsymbol{\mathcal{B}}}^{xc}$ to define the local torque of the xc magnetic field $\underline{\boldsymbol{\tau}_{xc}}$ as follows:[18,39,40]

$$\underline{\boldsymbol{\tau}_{xc}}(\underline{\mathbf{r}}) = \underline{\mathbf{m}}(\underline{\mathbf{r}}) \times \underline{\boldsymbol{\mathcal{B}}}^{xc}(\underline{\mathbf{r}}) \; . \tag{18}$$

The variables $\underline{\mathbf{Q}}$ on which the functional depends can in general be chosen such that the $\underline{\boldsymbol{\tau}_{xc}}$ is locally non-vanishing, even though in general its integral over all space $\int \underline{\boldsymbol{\tau}_{xc}}(\underline{\mathbf{r}}) d\underline{\mathbf{r}}$ should be null, such that it obeys the so-called zero-torque theorem.[18,39,40]

The Kohn-Sham Hamiltonian matrix elements are expressed using mono-electronic (including SR and SOC) and bi-electronic (Coulomb and exchange) integrals, as well as the xc potential $\hat{\mathbf{V}}_{xc}$ introduced above. For the diagonal spin-blocks we have:

$$\begin{aligned}\left[H_{KS}^{\sigma\sigma}\right]_{\mu\nu} = \left[h^{\sigma\sigma}\right]_{\mu\nu} + \left[C^{\sigma\sigma}\right]_{\mu\nu} + a\left[K^{\sigma\sigma}\right]_{\mu\nu} \\ + (1-a)\left[V_x^{\sigma\sigma}\right]_{\mu\nu} + \left[V_{\text{corr}}^{\sigma\sigma}\right]_{\mu\nu} \; .\end{aligned} \tag{19}$$

For off-diagonal spin-blocks (i.e. for $\sigma \neq \sigma'$), all mono-electronic integrals apart from SOC ones are null, as well as the bi-electronic Coulomb integrals (as shown in Part I), so that we have:

$$\begin{aligned}\left[H_{KS}^{\sigma\sigma'}\right]_{\mu\nu} = \left[h_{\text{SO}}^{\sigma\sigma'}\right]_{\mu\nu} + a\left[K^{\sigma\sigma'}\right]_{\mu\nu} \\ + (1-a)\left[V_x^{\sigma\sigma'}\right]_{\mu\nu} + \left[V_{\text{corr}}^{\sigma\sigma'}\right]_{\mu\nu} \; .\end{aligned} \tag{20}$$

The xc potential is described in the following according to two competing theories: the collinear and non-collinear formalisms.[5–8,10–12,38] In the collinear formalism, the xc potential is built from an xc functional which only depends on the z component of the magnetization m_z, that is only the $\mathcal{B}_z^{xc}$ component of the xc magnetic field is non-vanishing in Eq. (15). In this case, the lack of x and y components of the magnetization implies that the system looses the rotational invariance of the energy (i.e. within the collinear formulation, the energy of the system may vary depending on its relative orientation with respect to the Cartesian frame). On the contrary, the non-collinear formalism makes use of all three Cartesian components of the magnetization, such that rotational invariance is ensured. More details are provided below in Sections II C and II D on the two theories.

C. Collinear Density Functional Theory

In the collinear formalism, the variables $\underline{\mathbf{Q}}$ entering the exchange-correlation functional depend only on the total density n and z component of the magnetization m_z, while the x and y components of the magnetization are set to zero. As a consequence, the x and y components of the xc magnetic field introduced in Eq. (17) must vanish. From Eq. (15), the xc potential thus reduces to:

$${}^{\text{col}}\hat{\mathbf{V}}_{xc}(\underline{\mathbf{r}}) \; = \; {}^{\text{col}}\mathcal{E}^{xc}(\underline{\mathbf{r}})\hat{\boldsymbol{\sigma}}_0 \; + \; {}^{\text{col}}\mathcal{B}_z^{xc}(\underline{\mathbf{r}})\hat{\boldsymbol{\sigma}}_z \; . \tag{21}$$

Given the real nature of both $\hat{\boldsymbol{\sigma}}_0$ and $\hat{\boldsymbol{\sigma}}_z$, the xc potential therefore forms a real diagonal matrix in spin-space:

$${}^{\text{col}}\mathbf{V}_{xc} = \begin{pmatrix} {}^{\text{col}}\mathbf{V}_{xc}^{\alpha\alpha} & \mathbf{0}^{\alpha\beta} \\ \mathbf{0}^{\beta\alpha} & {}^{\text{col}}\mathbf{V}_{xc}^{\beta\beta} \end{pmatrix} \; , \tag{22}$$

whose matrix elements are real Hermitian:

$$\left[{}^{\text{col}}V_{xc}^{\sigma\sigma}\right]_{\mu\nu} \; = \; \left[{}^{\text{col}}V_{xc}^{\sigma\sigma}\right]_{\nu\mu}^{*} \; . \tag{23}$$

From Eq. (21) and by recalling the definition of the xc electrostatic potential and xc magnetic field given in Eqs. (16) and (17), we get the following expressions for the collinear xc potential in terms of functional derivatives of the collinear xc energy E_{xc}^{col} with respect to variables $n_+(\underline{\mathbf{r}})$ and $n_-(\underline{\mathbf{r}})$:

$${}^{\text{col}}\hat{V}_{xc}^{\alpha\alpha}(\underline{\mathbf{r}}) = \frac{\delta E_{xc}^{\text{col}}}{\delta n_+(\underline{\mathbf{r}})} \tag{24}$$

$${}^{\text{col}}\hat{V}_{xc}^{\beta\beta}(\underline{\mathbf{r}}) = \frac{\delta E_{xc}^{\text{col}}}{\delta n_-(\underline{\mathbf{r}})} \; . \tag{25}$$

The main advantage of the collinear formalism is that little modifications of the non- or scalar-relativistic part of an existing code that calculates the xc energy and the xc potential matrix elements within a one-component approach are necessary to implement this theory. Moreover, xc functionals made for non-relativistic calculations can be used in exactly the same way as they were devised.

The disadvantage of the collinear theory is that rotational invariance is lost when calculations are performed in the presence of a SOC operator. The loss of rotational invariance means that a rigid rotation of the molecule will cause a change in energy. This occurs because the collinear theory effectively consists of choosing the spin-quantisation axis along z for the xc potential term. Given that the SOC operator imparts an energy dependence on the orientation of the spin-quantisation axis,[31] the arbitrary and non-general choice of the z direction results in loss of rotational invariance.

1. Collinear LDA

As introduced in Section II B, LDA xc functionals only depend on $n_+(\underline{\mathbf{r}})$ and $n_-(\underline{\mathbf{r}})$, which, in the collinear formalism (in analogy to the non- or scalar-relativistic one-component approach), are defined as:

$$n_+^{\text{col}}(\underline{\mathbf{r}}) = n_{\alpha\alpha}^{\Re}(\underline{\mathbf{r}}) \tag{26}$$

$$n_-^{\text{col}}(\underline{\mathbf{r}}) = n_{\beta\beta}^{\Re}(\underline{\mathbf{r}}) \; , \tag{27}$$

and are therefore built solely from the real part of the $\alpha\alpha$ and $\beta\beta$ blocks of the density matrix. The superscript "col" indicates that these are the definitions of $n_\pm$ specific to the collinear formalism. From Eqs. (6) and (9), the variables above can be shown to depend only on the total density n and z component of the magnetization m_z as:

$$n_\pm^{\text{col}}(\underline{\mathbf{r}}) = \frac{1}{2}\left[n(\underline{\mathbf{r}}) \pm m_z(\underline{\mathbf{r}})\right] \; . \tag{28}$$

From calculus of variations, for LDA, the functional derivatives of the energy in Eqs. (24) and (25) reduce to the following partial derivatives of the xc functional:

$$^{\rm col}\hat{V}^{\sigma\sigma}_{xc}(\underline{\mathbf{r}}) = \frac{\partial F^{\rm col}_{xc}}{\partial n^{\Re}_{\sigma\sigma}(\underline{\mathbf{r}})} \; . \tag{29}$$

2. Collinear GGA and Hybrids

As discussed above, apart from the $n_\pm$ introduced above, GGA xc functionals (and GGA hybrids) also depend on gradient variables $\gamma_{\pm\pm}$, which, within the collinear formalism (again, in analogy to the non-relativistic one-component approach), are defined as:

$$\gamma^{\rm col}_{\pm\pm}(\underline{\mathbf{r}}) = \underline{\hat{\boldsymbol{\nabla}}} n^{\rm col}_{\pm}(\underline{\mathbf{r}}) \cdot \underline{\hat{\boldsymbol{\nabla}}} n^{\rm col}_{\pm}(\underline{\mathbf{r}}) \; . \tag{30}$$

From Eq. (28), it is easy to see that also these variables only depend on the total density n and z component of the magnetization m_z:

$$\gamma^{\rm col}_{\pm\pm}(\underline{\mathbf{r}}) = \frac{1}{4}\underline{\hat{\boldsymbol{\nabla}}} \left[n(\underline{\mathbf{r}}) \pm m_z(\underline{\mathbf{r}})\right] \cdot \underline{\hat{\boldsymbol{\nabla}}} \left[n(\underline{\mathbf{r}}) \pm m_z(\underline{\mathbf{r}})\right] \tag{31}$$

For GGA, standard calculus of variations gives the following expression for the xc potential:[41]

$$^{\rm col}\hat{V}^{\sigma\sigma}_{xc}(\underline{\mathbf{r}}) = \frac{\partial F^{col}_{xc}}{\partial n^{\Re}_{\sigma\sigma}(\underline{\mathbf{r}})} - \underline{\hat{\boldsymbol{\nabla}}} \cdot \left[2 \frac{\partial F^{col}_{xc}}{\partial \left| \underline{\hat{\boldsymbol{\nabla}}} n^{\Re}_{\sigma\sigma}(\underline{\mathbf{r}}) \right|^2} \underline{\hat{\boldsymbol{\nabla}}} n^{\Re}_{\sigma\sigma}(\underline{\mathbf{r}}) + \frac{\partial F^{col}_{xc}}{\partial \gamma^{col}_{+-}(\underline{\mathbf{r}})} \underline{\hat{\boldsymbol{\nabla}}} n^{\Re}_{\sigma'\sigma'}(\underline{\mathbf{r}}) \right] , \tag{32}$$

where in the equation above $\sigma \neq \sigma'$. From Eq. (32), for GGA functionals the evaluation of the xc potential would require the second derivatives of the xc functional. However, as was first noted by Pople and co-workers,[41] the evaluation of the xc potential is actually not necessary, because we are only interested in the evaluation of the matrix elements of the xc potential and these can be obtained through integration by parts, such that only the first derivatives of the functional are required, as follows:

$$\left[^{\rm col}V^{\sigma\sigma}_{xc}\right]_{\mu\nu} = \int \frac{\partial F^{col}_{xc}}{\partial n^{\Re}_{\sigma\sigma}(\underline{\mathbf{r}})} \chi_\mu(\underline{\mathbf{r}})\chi_\nu(\underline{\mathbf{r}}) d\underline{\mathbf{r}} \; + \; \int \left[2 \frac{\partial F^{col}_{xc}}{\partial \left| \underline{\hat{\boldsymbol{\nabla}}} n^{\Re}_{\sigma\sigma}(\underline{\mathbf{r}}) \right|^2} \underline{\hat{\boldsymbol{\nabla}}} n^{\Re}_{\sigma\sigma}(\underline{\mathbf{r}}) + \frac{\partial F^{col}_{xc}}{\partial \gamma^{col}_{+-}(\underline{\mathbf{r}})} \underline{\hat{\boldsymbol{\nabla}}} n^{\Re}_{\sigma'\sigma'}(\underline{\mathbf{r}}) \right] \cdot \underline{\hat{\boldsymbol{\nabla}}} \chi_\mu(\underline{\mathbf{r}})\chi_\nu(\underline{\mathbf{r}}) d\underline{\mathbf{r}} \tag{33}$$

D. Non-Collinear Density Functional Theory

In the non-collinear formalism, the variables entering the exchange-correlation functional depend on the total density n and on the three Cartesian components of the magnetization $\underline{\mathbf{m}}$, so that rotational invariance is ensured even in the presence of the SOC operator. Therefore, from Eqs. (6) - (9), the xc functional depends on all blocks of the density matrix apart form $\Im\mathbf{D}^{\alpha\alpha}$ and $\Im\mathbf{D}^{\beta\beta}$. We note in passing that these latter blocks enter the definition of the orbital current density that thus would not be correctly described. However, we also note that the inclusion of a fraction of Fock exchange, as done in hybrid functionals, introduces the missing dependence on these blocks of the density matrix and therefore allows to better describe the orbital current density.

Given that the xc functional now depends on the total density and on the three Cartesian components of the magnetization, the non-collinear xc potential has the form shown on Eq. (15) and therefore forms a complex matrix in spin-space:

$$\mathbf{V}_{xc} = \begin{pmatrix} \mathbf{V}^{\alpha\alpha}_{xc} & \mathbf{V}^{\alpha\beta}_{xc} \\ \mathbf{V}^{\beta\alpha}_{xc} & \mathbf{V}^{\beta\beta}_{xc} \end{pmatrix} \; . \tag{34}$$

Based on Eq. (15) and on the expressions for the Pauli matrices, the following symmetry properties can be derived. For the diagonal $\alpha\alpha$ spin-block:

$$\begin{aligned} \left[V^{\alpha\alpha}_{xc}\right]_{\mu\nu} &= \left[V^{\alpha\alpha}_{xc}\right]_{\nu\mu} \\ &= \langle\chi_\mu|\mathcal{E}^{xc} + \mathcal{B}^{xc}_z|\chi_\nu\rangle \; . \end{aligned} \tag{35}$$

For the diagonal $\beta\beta$ spin-block:

$$\begin{aligned} \left[V^{\beta\beta}_{xc}\right]_{\mu\nu} &= \left[V^{\beta\beta}_{xc}\right]_{\nu\mu} \\ &= \langle\chi_\mu|\mathcal{E}^{xc} - \mathcal{B}^{xc}_z|\chi_\nu\rangle \; . \end{aligned} \tag{36}$$

For the off-diagonal spin-blocks, the matrix elements read as follows:

$$\begin{aligned} \left[V^{\alpha\beta}_{xc}\right]_{\mu\nu} = \left[V^{\alpha\beta}_{xc}\right]_{\nu\mu} &= \left[V^{\beta\alpha}_{xc}\right]^*_{\nu\mu} = \left[V^{\beta\alpha}_{xc}\right]^*_{\mu\nu} \\ &= \langle\chi_\mu|\mathcal{B}^{xc}_x - i\mathcal{B}^{xc}_y|\chi_\nu\rangle \; . \end{aligned} \tag{37}$$

So the diagonal $\alpha\alpha$ and $\beta\beta$ spin-blocks of the xc potential are real Hermitian so that only their upper (or lower) triangular parts need to be computed. The off-diagonal $\alpha\beta$ and $\beta\alpha$ spin-blocks are complex symmetric so that only the upper (or lower) triangular part of $\alpha\beta$ needs to be calculated.

Depending on the choice of the variables used in the definition of the xc functional, several formulations of non-collinear two-component DFT are possible. We are going to review existing ones and present a new formulation below, which is characterized by a higher numerical stability.

1. The Canonical Formulation

In the canonical formulation of the non-collinear DFT, the variables on which F_{xc} depends are built starting from the generalized density:[5]

$$\bar{\mathbf{n}}(\underline{\mathbf{r}}) = \frac{1}{2}\left[n(\underline{\mathbf{r}})\hat{\boldsymbol{\sigma}}_0 + \sum_c m_c(\underline{\mathbf{r}})\hat{\boldsymbol{\sigma}}_c\right] . \tag{38}$$

By recalling the exact form of the Pauli matrices given in Eq. (4) of Part I, the generalized density can be written explicitly as follows in terms of the total density and components of the magnetization:

$$\bar{\mathbf{n}}(\underline{\mathbf{r}}) = \frac{1}{2}\begin{pmatrix} n(\underline{\mathbf{r}}) + m_z(\underline{\mathbf{r}}) & m_x(\underline{\mathbf{r}}) - im_y(\underline{\mathbf{r}}) \\ m_x(\underline{\mathbf{r}}) + im_y(\underline{\mathbf{r}}) & n(\underline{\mathbf{r}}) - m_z(\underline{\mathbf{r}}) \end{pmatrix} . \tag{39}$$

By performing a unitary transformation on the generalized density $\bar{\mathbf{n}}$, which diagonalizes locally in space the matrix above, one gets the $n_\pm$ variables used in the definition of the xc functional:[6]

$$\bar{\mathbf{n}}(\underline{\mathbf{r}}) \overset{diag}{=} \begin{pmatrix} n_+(\underline{\mathbf{r}}) & 0 \\ 0 & n_-(\underline{\mathbf{r}}) \end{pmatrix} , \tag{40}$$

where the eigenvalues of the matrix are:

$$n_\pm(\underline{\mathbf{r}}) = \frac{1}{2}\left[n(\underline{\mathbf{r}}) \pm m(\underline{\mathbf{r}})\right] , \tag{41}$$

where $m = |\underline{\mathbf{m}}|$ is the magnitude of $\underline{\mathbf{m}}$. Comparison of Eq. (41) with Eqs. (26) and (27), shows that the non-collinear definition of the $n_\pm$ variables differs from the collinear definition by replacing m_z by m (i.e. the z component of the magnetization by the absolute value of the magnetization).

From the definitions of the xc electrostatic potential and magnetic field given in Eqs. (16) and (17) in terms of $n_\pm$ and from the expressions of $n_\pm$ derived in Eq. (41), we can express the xc electrostatic potential and magnetic field as functional derivatives of the xc energy with respect to the generalized density and magnetization, respectively:

$$\mathcal{E}^{xc} = \frac{1}{2}\frac{\delta E_{xc}}{\delta n} ; \tag{42}$$

$$\mathcal{B}_c^{xc} = \frac{1}{2}\frac{\delta E_{xc}}{\delta m_c} = \frac{m_c}{2m}\frac{\delta E_{xc}}{\delta m} , \tag{43}$$

where from now on the dependence on $\underline{\mathbf{r}}$ is dropped, and where in the above we have used the fact that, from the chain rule of differentiation:

$$\frac{\delta E_{xc}}{\delta m_c} = \frac{\delta E_{xc}}{\delta m}\frac{\delta m}{\delta m_c} = \frac{\delta E_{xc}}{\delta m}\frac{m_c}{m} . \tag{44}$$

From Eq. (43) we see that the xc potential is parallel to the magnetization. Finally, comparison of Eq. (15) for the xc potential with Eq. (38) for the generalized density, and use of the equalities in Eqs. (42) and (43), shows that the xc potential operator can be written more succinctly as a functional derivative of the xc energy with respect to the generalized density:

$$\hat{\mathbf{V}}_{xc} = \frac{\delta E_{xc}}{\delta \bar{\mathbf{n}}} . \tag{45}$$

When considering an LDA xc functional, the functional derivatives of the xc energy in Eqs. (42) and (43) reduce to partial derivatives of the xc functional:

$$\mathcal{E}^{xc} = \frac{1}{2}\frac{\partial F_{xc}}{\partial n} \quad ; \quad \mathcal{B}_c^{xc} = \frac{m_c}{2m}\frac{\partial F_{xc}}{\partial m} . \tag{46}$$

In a scalar- or non-relativistic code, the partial derivatives of the xc functional with respect to n and m_z are available. So, for an LDA functional, one has to simply replace m_z by m in the existing code to generalize it to the canonical non-collinear theory.

GGA xc functionals also depend on the gradient variables $\gamma_{\pm\pm}$ that, within the canonical formulation of non-collinear DFT read:

$$\gamma_{\pm\pm} = \frac{1}{4}\left\{\underline{\hat{\boldsymbol{\nabla}}}\left[n \pm m\right] \cdot \underline{\hat{\boldsymbol{\nabla}}}\left[n \pm m\right]\right\} , \tag{47}$$

where the gradient of the absolute magnetization is calculated as follows:

$$\underline{\hat{\boldsymbol{\nabla}}} m = \frac{1}{m}\sum_c m_c \underline{\hat{\boldsymbol{\nabla}}} m_c . \tag{48}$$

Later we are going to discuss some numerical issues and corresponding solutions related to the treatment of these terms. For application to GGA functionals, standard calculus of variations leads to the following expressions for the functional derivatives of the xc energy in Eqs. (42) and (43):

$$\mathcal{E}^{xc} = \frac{1}{2}\Bigg\{ \underbrace{\left(\frac{\partial F_{xc}}{\partial n_+} + \frac{\partial F_{xc}}{\partial n_-}\right)}_{\Gamma_+} - \underline{\hat{\boldsymbol{\nabla}}} \cdot \underbrace{\left[2\frac{\partial F_{xc}}{\partial \gamma_{++}} \underline{\hat{\boldsymbol{\nabla}}} n_+ + 2\frac{\partial F_{xc}}{\partial \gamma_{--}} \underline{\hat{\boldsymbol{\nabla}}} n_- + \frac{\partial F_{xc}}{\partial \gamma_{+-}} \left(\underline{\hat{\boldsymbol{\nabla}}} n_+ + \underline{\hat{\boldsymbol{\nabla}}} n_- \right) \right]}_{\Lambda_+} \Bigg\} ; \tag{49}$$

and:

$$\mathcal{B}_c^{xc} = \frac{m_c}{2m}\Bigg\{ \underbrace{\left(\frac{\partial F_{xc}}{\partial n_+} - \frac{\partial F_{xc}}{\partial n_-}\right)}_{\Gamma_-} - \underline{\hat{\boldsymbol{\nabla}}} \cdot \underbrace{\left[2\frac{\partial F_{xc}}{\partial \gamma_{++}} \underline{\hat{\boldsymbol{\nabla}}} n_+ - 2\frac{\partial F_{xc}}{\partial \gamma_{--}} \underline{\hat{\boldsymbol{\nabla}}} n_- - \frac{\partial F_{xc}}{\partial \gamma_{+-}} \left(\underline{\hat{\boldsymbol{\nabla}}} n_+ - \underline{\hat{\boldsymbol{\nabla}}} n_- \right) \right]}_{\Lambda_-} \Bigg\} . \tag{50}$$

From Eqs. (35), (36) and (37), we see that the matrix elements of the GGA xc potential are built from $\left[\mathcal{E}^{xc}\right]_{\mu\nu}$ and $\left[\mathcal{B}_c^{xc}\right]_{\mu\nu}$. Through integration by parts, we find the following working expressions:

$$\left[\mathcal{E}^{xc}\right]_{\mu\nu} = \frac{1}{2}\left[\int \chi_\mu \chi_\nu \Gamma_+ d\underline{\mathbf{r}} + \int \Lambda_+ \cdot \underline{\hat{\boldsymbol{\nabla}}} \left(\chi_\mu \chi_\nu\right) d\underline{\mathbf{r}} \right] , \tag{51}$$

and:

$$\left[\mathcal{B}_c^{xc}\right]_{\mu\nu} = \int \frac{m_c}{2m} \chi_\mu \chi_\nu \Gamma_- d\underline{\mathbf{r}} + \int \frac{m_c}{2m} \Lambda_- \cdot \underline{\hat{\boldsymbol{\nabla}}} \left(\chi_\mu \chi_\nu\right) d\underline{\mathbf{r}} . \tag{52}$$

In the end, the canonical formulation of the non-collinear DFT works in terms of the n and m variables (and their gradients for GGA functionals), at variance with the standard non-relativistic one-component theory where the variables n and m_z are used. The expressions for the matrix elements derived above are somewhat similar to the corresponding Eqs. (32) and (33) for the collinear approach described before. The major difference is that, in the canonical non-collinear approach, the $n_\pm$ and $\gamma_{\pm\pm}$ are built using the absolute value m of the magnetization $\underline{\mathbf{m}}$. Thus, also m_x and m_y Cartesian components of the magnetization are needed.

2. The Scalmani-Frisch Formulation

Scalmani and Frisch have proposed an alternative formulation of the non-collinear theory, which differs from the canonical theory illustrated above for functionals beyond the LDA.[9] This theory adopts the following definitions for the GGA variables:

$$\begin{aligned} \bar{\gamma}_{++} \text{ or } \bar{\gamma}_{--} = & \frac{1}{4}\left[\underline{\hat{\boldsymbol{\nabla}}} n \cdot \underline{\hat{\boldsymbol{\nabla}}} n + \underline{\hat{\boldsymbol{\nabla}}}\ \underline{\mathbf{m}} \cdot \circ \underline{\hat{\boldsymbol{\nabla}}}\ \underline{\mathbf{m}} \right] \\ & \pm \frac{f_\nabla}{2} \underbrace{\left[\left(\underline{\hat{\boldsymbol{\nabla}}} n \cdot \underline{\hat{\boldsymbol{\nabla}}}\ \underline{\mathbf{m}} \right) \circ \left(\underline{\hat{\boldsymbol{\nabla}}} n \cdot \underline{\hat{\boldsymbol{\nabla}}}\ \underline{\mathbf{m}} \right) \right]^{\frac{1}{2}}}_{\Xi} \end{aligned} \tag{53}$$

and:

$$\bar{\gamma}_{+-} = \frac{1}{4}\left[\underline{\hat{\boldsymbol{\nabla}}} n \cdot \underline{\hat{\boldsymbol{\nabla}}} n - \underline{\hat{\boldsymbol{\nabla}}}\ \underline{\mathbf{m}} \cdot \circ \underline{\hat{\boldsymbol{\nabla}}}\ \underline{\mathbf{m}} \right] , \tag{54}$$

where the bar accent indicates that these are the corresponding definitions of the $\gamma_{\pm\pm}$ variables introduced in Eq. (13). In this section, the dot product identified by the symbol "$\cdot$" runs over the components of $\underline{\hat{\boldsymbol{\nabla}}}$ while that identified by the symbol "$\circ$" runs over the components of $\underline{\mathbf{m}}$. Finally, the f_∇ is defined as:

$$f_\nabla = \mathrm{sgn}\left[\underline{\hat{\boldsymbol{\nabla}}} n \cdot \left(\underline{\hat{\boldsymbol{\nabla}}}\ \underline{\mathbf{m}} \right) \circ \underline{\mathbf{m}} \right] , \tag{55}$$

where the signum function "sgn" returns either 1 or -1 according to the sign of the argument. We obtain expressions for the matrix elements of the theory of Scalmani and Frisch from the calculus of variations. We do not show details of the derivation, but report the final expressions, as follows:

$$\begin{aligned} \left[\bar{\mathcal{E}}^{xc}\right]_{\mu\nu} = & \frac{1}{2}\int \Gamma_+ \chi_\mu \chi_\nu d\underline{\mathbf{r}} + \frac{1}{2}\int \Bigg\{ \left(\frac{\partial F_{xc}}{\partial \bar{\gamma}_{++}} + \frac{\partial F_{xc}}{\partial \bar{\gamma}_{--}} + \frac{\partial F_{xc}}{\partial \bar{\gamma}_{+-}} \right) \underline{\hat{\boldsymbol{\nabla}}} n \\ & + \left(\frac{\partial F_{xc}}{\partial \bar{\gamma}_{++}} - \frac{\partial F_{xc}}{\partial \bar{\gamma}_{--}} \right) f_\nabla\, \Xi^{-1} \left(\underline{\hat{\boldsymbol{\nabla}}} n \cdot \underline{\hat{\boldsymbol{\nabla}}}\ \underline{\mathbf{m}} \right) \circ \underline{\hat{\boldsymbol{\nabla}}}\ \underline{\mathbf{m}} \Bigg\} \cdot \underline{\hat{\boldsymbol{\nabla}}} \left(\chi_\mu \chi_\nu\right) d\underline{\mathbf{r}} , \end{aligned} \tag{56}$$

and:

$$\begin{aligned} \left[\bar{\mathcal{B}}_c^{xc}\right]_{\mu\nu} = & \frac{1}{2}\int \frac{m_c}{m} \Gamma_- \chi_\mu \chi_\nu d\underline{\mathbf{r}} + \frac{1}{2}\int \Bigg\{ \left(\frac{\partial F_{xc}}{\partial \bar{\gamma}_{++}} + \frac{\partial F_{xc}}{\partial \bar{\gamma}_{--}} - \frac{\partial F_{xc}}{\partial \bar{\gamma}_{+-}} \right) \underline{\hat{\boldsymbol{\nabla}}} m_c \\ & + \left(\frac{\partial F_{xc}}{\partial \bar{\gamma}_{++}} - \frac{\partial F_{xc}}{\partial \bar{\gamma}_{--}} \right) f_\nabla\, \Xi^{-1} \left(\underline{\hat{\boldsymbol{\nabla}}} n \cdot \underline{\hat{\boldsymbol{\nabla}}} m_c \right) \underline{\hat{\boldsymbol{\nabla}}} n \Bigg\} \cdot \underline{\hat{\boldsymbol{\nabla}}} \left(\chi_\mu \chi_\nu\right) d\underline{\mathbf{r}} . \end{aligned} \tag{57}$$

3. The Signed Canonical Formulation

In this Section, we introduce a new formulation of non-collinear DFT, which represents a modification of the canonical approach described in Section II D 1 that ensures a better physical description of non-collinear magnetization and a higher numerical stability. As we will show, it turns out that such modification is necessary to guarantee rotational invariance and reduction to the proper collinear limit because these are otherwise not achieved with either the canonical or SF formulations for functionals beyond the LDA. We apply the modification to the canonical formulation, but in principle the same could be done for the SF formulation. In our modified version of the canonical non-collinear DFT, a new set of variables $\underline{\tilde{\mathbf{Q}}}$ is used in terms of which the xc functional is defined:

$$F_{xc}[\underline{\mathbf{Q}}] \rightarrow F_{xc}[\underline{\tilde{\mathbf{Q}}}] \; . \tag{58}$$

As we have discussed in Section II D 1, when passing from the collinear formulation to the canonical non-collinear formulation, the z component of the magnetization m_z is locally substituted by the absolute value of the magnetization $m = |\underline{\mathbf{m}}|$ (i.e. a quantity that also depends on the m_x and m_y components of the magnetization), which formally ensures the rotational invariance to the theory for LDA functionals.

The new set of variables $\underline{\tilde{\mathbf{Q}}}$ is here found by first identifying the problems associated with the canonical theory. These arise from loss of information on the local sign of the magnetization in the definition of the gradient variables $\gamma_{\pm\pm}$ of Eq. (47) needed for GGA functionals. In particular, the problem is due to the sign of the gradient of the absolute value of the magnetization $\underline{\hat{\boldsymbol{\nabla}}} m$, introduced in Eq. (48), that is the variable that substitutes $\underline{\hat{\boldsymbol{\nabla}}} m_z$ when passing from the collinear to the canonical non-collinear theory. In the collinear formulation, the sign of $\underline{\hat{\boldsymbol{\nabla}}} m_z$ coincides with the sign of the gradient of the z component of the magnetization. On the contrary, from Eq. (48), in the canonical non-collinear theory, the sign of $\underline{\hat{\boldsymbol{\nabla}}} m$ does not only depend on the sign of the gradients of the Cartesian components of the magnetization $\underline{\hat{\boldsymbol{\nabla}}} m_c$ but also on the sign of the Cartesian components themselves m_c. This implies, for example, that at a given point in space where the gradients of the three Cartesian components of the magnetization are all positive (i.e. $\underline{\hat{\boldsymbol{\nabla}}} m_c > 0$ for $c = x, y, z$), the sign of the variable $\underline{\hat{\boldsymbol{\nabla}}} m$ will not necessarily be positive, if some of the m_c are negative. For the terms in Eq. (43), where we have factors of m_c/m, a similar problem occurs if the m has a different sign than that of m_c.

As a consequence of this inconsistency of signs, the canonical non-collinear theory does not yield the same solution as the collinear theory in the limit where the magnetization is everywhere parallel (the collinear limit), for GGA functionals. The canonical non-collinear theory also suffers from SCF instabilities and slow convergence as a result of the gradient variables having the wrong sign. All of these issues of the canonical formulation, some of which have been acknowledged before,[9] are going to be discussed in Section IV.

We call our modified version of the theory, "signed canonical non-collinear DFT". The new variables $\underline{\tilde{\mathbf{Q}}}$ on which the xc functional F_{xc} depends are defined as follows:

$$\tilde{n}_{\pm} = \frac{1}{2}\left(n \pm \tilde{m}\right) \; ; \tag{59}$$

$$\tilde{\gamma}_{\pm\pm} = \frac{1}{4}\left[\left(\underline{\hat{\boldsymbol{\nabla}}} n \pm \underline{\boldsymbol{\xi}}\right) \cdot \left(\underline{\hat{\boldsymbol{\nabla}}} n \pm \underline{\boldsymbol{\xi}}\right)\right] \; , \tag{60}$$

where:

$$\tilde{m} = \mathrm{sgn}\left(m_x + m_y + m_z\right) m \; ; \tag{61}$$

$$\underline{\boldsymbol{\xi}} = \frac{1}{m}\sum_c |m_c| \, \underline{\hat{\boldsymbol{\nabla}}} m_c \; . \tag{62}$$

The new variables $\tilde{n}_{\pm}$ and $\tilde{\gamma}_{\pm\pm}$ therefore only differ from the canonical variables $n_{\pm}$ and $\gamma_{\pm\pm}$ on how the sign is chosen for the magnetization and the gradient of the magnetization. These new signs follow the sign of the Cartesian components m_c and their gradients $\underline{\hat{\boldsymbol{\nabla}}} m_c$ locally in space. This implies that, by using the new variables, the correct collinear limit can be obtained even for GGA functionals, and the SCF is now devoid of instabilities and convergence problems related to wrong signs of the gradient variables. With the new variables, the expressions for the xc potential are only slightly modified from those provided in Section II D 1 for the unmodified canonical theory. The only difference is that now in Eq. (43) some factors are replaced as follows:

$$m_c \frac{\delta E_{xc}}{\delta m} \rightarrow |m_c| \, \frac{\delta E_{xc}}{\delta m} \; . \tag{63}$$

Therefore, from Eq. (52), the xc magnetic field matrix elements now read:

$$\left[\tilde{\mathcal{B}}_c^{xc}\right]_{\mu\nu} = \int \frac{|m_c|}{2m} \chi_\mu \chi_\nu \Gamma_- d\underline{\mathbf{r}} + \int \frac{|m_c|}{2m} \Lambda_- \cdot \underline{\hat{\boldsymbol{\nabla}}} \left(\chi_\mu \chi_\nu\right) d\underline{\mathbf{r}} \; . \tag{64}$$

Otherwise, the electrostatic potential matrix elements are equivalent to those from the canonical approach.

Let us stress that our modified version of the theory is exact (as regards accounting for the local sign of the magnetization) for all those cases in which, at each point in space, the non-zero Cartesian components of the magnetization have the same sign. That is to say, the signed canonical theory can deal exactly with some points in space where, say, m_x and m_z are both positive while m_y is zero, and other points in space where m_y and m_z are both negative while m_x is zero. We note that the modified theory is not exact if there are points where the magnetization has two relevant Cartesian components of different sign. However, this should not be too restrictive, as for most systems the orientation of the magnetization does not vary more than 90° throughout space, so that

often the system can be re-oriented so as to cope with this condition. Nevertheless, few exotic electronic structures, such as 3D spin-spirals, could not fully conform to this approach. We are going to discuss this point in Section IV below.

4. On the Treatment of Unstable Terms of Non-Collinear Exchange-Correlation Potentials

We discuss here algorithmic strategies for the evaluation of delicate terms in the non-collinear xc potential. Several previous authors have acknowledged numerical issues associated with the evaluation of non-collinear xc potentials, particularly so for xc functionals beyond the LDA.[6–12,15,40] However, to the best of our knowledge, an effective screening algorithm for dealing with these problems is yet to be presented in the literature.

All of the difficulties previously noted in the literature are related to factors $R_c = m_c/m$, which are ill-defined at those points in space where the magnetization is small. In general, these factors appear both in the expressions for the variables on which GGA xc functionals depend and in the expression for the xc magnetic field (for all functionals, including LDA). In the canonical and signed-canonical theories, the challenging terms occur in both the definition of the GGA variables – see Eq. (48) for the canonical theory and Eq. (62) for the signed-canonical theory – and in the xc potential, see Eq. (52) and Eq. (64), respectively. For the theory of Scalmani and Frisch, the problematic terms do not occur in the definition of the GGA variables, but are still present in the definition of the xc magnetic field term of the potential in Eq. (57).

For LDA functionals, points of small magnetization can be safely disregarded because the m_c/m factors in the potential multiply other terms which are also vanishing for vanishing m. This is not the case for GGA functionals, where the m_c/m (or $|m_c|/m$ in the signed-canonical theory) factors sometimes multiply gradients of the magnetization, gradients of the total density, or gradients of the atomic orbitals, which are not necessarily small where m is small. See for example Eqs. (48) and (52) for the canonical theory.

As a consequence, the treatment of these terms requires a very careful local screening of the magnitude of the magnetization m and of its individual Cartesian components m_c at each point of the DFT grid. Here we introduce a screening algorithm that can be used with any non-collinear formulation and sketch its main features. The algorithm is presented for the case where the m_c/m terms multiply gradients of the magnetization in the canonical theory but it can be very easily extended to the cases where the m_c/m (or $|m_c|/m$ in the case of the signed-canonical theory) factors multiply instead gradients of the total density or gradients of the atomic orbitals.

At each point in space (i.e. at each point of the DFT integration grid), the absolute value $|m_c|$ of the three Cartesian components of the magnetization $\underline{\mathbf{m}}$ are screened according to a threshold (here set to 10^{-14} a.u.). Two distinct cases are identified and treated differently: 1) all three components are individually smaller than the threshold, or 2) at least one component is larger than the threshold. We treat these two cases as follows:

1. The three components of the magnetization are all small. We locally set:

$$\begin{aligned} m &= 0 \; ; \\ \hat{\underline{\nabla}} m &= \sum_c \left\langle \frac{m_c}{m} \right\rangle \hat{\underline{\nabla}} m_c \; , \end{aligned}$$

   where the gradient of the magnetization $\hat{\underline{\nabla}} m$ at that point is expressed in terms of the gradients of the three Cartesian components of the magnetization at the same point $\hat{\underline{\nabla}} m_c$ while the prefactors $\langle m_c/m \rangle$ are average values for m_c/m over the atomic basin to which the point belongs.[42] These average values are essential to ensure numerical stability at those (many) points where the m_c and m are so small that their ratio could not be evaluated with any reasonable degree of confidence. Moreover, they are also useful when m_c is too small to reasonably determine its sign (positive or negative). For these reasons, it is beneficial to instead associate an average value to m_c/m calculated over the atomic basin of the current point in space.

2. At least one of the three Cartesian components of the magnetization is large in absolute value. The largest component, in absolute value, is determined and the following signed quantity defined:

$$\begin{aligned} m_{max} = &\operatorname{sgn}\left(m_x + m_y + m_z\right) \\ &\times \max\left(\left|m_x\right|, \left|m_y\right|, \left|m_z\right|\right) \; . \end{aligned}$$

   At this point, a screening on the "local collinearity" is performed. The absolute value of the other two, non-maximum, components of the magnetization is checked relative to $|m_{max}|$. Two distinct cases are identified, which are treated differently:

   (a) Both non-maximum Cartesian components are small relative to $|m_{max}|$ and therefore the system is locally collinear. The two small components are put to zero and the problem reduces to the collinear one with the quantization axis along $|m_{max}|$. In this case we set:

$$\begin{aligned} m &= |m_{max}| \; , \\ \hat{\underline{\nabla}} m &= \operatorname{sgn}(m_{max}) \hat{\underline{\nabla}} m_{max} \; . \end{aligned}$$

   (b) At least one of the non-maximum Cartesian components is not small relative to $|m_{max}|$. In

this case, we set explicitly:

$$m = \sqrt{m_x^2 + m_y^2 + m_z^2} \, ,$$
$$\underline{\hat{\mathbf{\nabla}}} m = \sum_c R_c \underline{\hat{\mathbf{\nabla}}} m_c \, ,$$

where the factors R_c are determined as follows, based on the value of the ratios $|m_c|/m$: if the ratio $|m_c|/m$ is small than we set $R_c = 0$, otherwise we set it to $R_c = m_c/m$.

We note that the use of this screening algorithm ensures a better numerical stability to all non-collinear formulations discussed in Section II D. In the context of the canonical and Scalmani-Frisch formulations, it is key to correctly account for both the sign and magnitude of the ratios m_c/m. In our "signed canonical" theory, the sign of those terms is already taken into explicit account so that the quantities of interest are the ratios $|m_c|/m$, which are always positive. The algorithm illustrated above still allows to effectively screen these terms based on their magnitude.

Based on our experience, the majority of the numerical issues of non-collinear potentials arise from local inconsistencies in the sign of the m_c/m ratios, and to a lower extent in their magnitude. As a result, a combination of the above proposed screening algorithm with the "signed canonical" theory illustrated in Section II D 3 results in a very stable implementation, as will be shown in Section IV.

III. COMPUTATIONAL DETAILS

We have implemented all of the DFT formulations discussed above in a developmental version of the CRYSTAL17 code.[32] To validate our implementation and discuss numerical strategies for its use, we have chosen a test set of small molecular systems, and have performed similar calculations also with the latest public version of the DIRAC[43] and TURBOMOLE[44] codes. In contrast to Part I, here we cannot perform comparisons with the NWCHEM code,[36,45] because it appears that unlike our implementation, their calculation of the xc energy follows a prescription which is inconsistent with the original formulation of Hohenberg and Kohn.[46] The systems are similar to those discussed in Part I.[31] That is, the I_2, CH_3I, IH and TlBr molecules, in both a neutral state (closed-shell electronic configurations) and a positively charged state obtained by removing one electron from the molecules (open-shell electronic configurations): namely, I_2^+, CH_3I^+, IH^+ and $TlBr^+$. We refer the reader to Part I for details on the used basis sets, ECPs and molecular geometries.

The numerical integration required for calculating the xc energy and matrix elements was achieved with our implementation on an unpruned grid containing 75 radial points and a Lebedev accuracy level of 16, corresponding to 974 angular point for each radial point.[47–49]

TABLE I. Energies for the closed-shell electronic configurations. The $\Delta E_{SOC} = E_{SOC} - E_0$ is the SOC contribution to the energy as obtained with our implementation. The $\Delta\Delta E_X = \Delta E_X - \Delta E_{SOC}$ is the difference between the SOC energy contribution computed with the program X=TUR or DIR (where TUR stands for TURBOMOLE and DIR stands for DIRAC) and that with our implementation. All quantities are reported in atomic units (Ha).

	I_2	CH_3I	IH	TlBr
LDA				
ΔE_{SOC}	-7.7×10^{-3}	-3.2×10^{-3}	-3.0×10^{-3}	-3.6×10^{-2}
$\Delta\Delta E_{DIR}$	$+4.8\times10^{-9}$	$+4.0\times10^{-9}$	$+1.0\times10^{-9}$	-
$\Delta\Delta E_{TUR}$	$+1.2\times10^{-5}$	$+1.3\times10^{-6}$	$+6.9\times10^{-7}$	$+2.6\times10^{-6}$
PBE				
ΔE_{SOC}	-7.9×10^{-3}	-3.2×10^{-3}	-3.0×10^{-3}	-3.5×10^{-2}
$\Delta\Delta E_{DIR}$	$+1.3\times10^{-8}$	$+1.8\times10^{-9}$	$+2.1\times10^{-9}$	-
$\Delta\Delta E_{TUR}$	$+1.4\times10^{-5}$	$+1.4\times10^{-6}$	$+2.9\times10^{-7}$	$+2.5\times10^{-6}$
PBE0				
ΔE_{SOC}	-7.7×10^{-3}	-3.1×10^{-3}	-2.9×10^{-3}	-3.4×10^{-2}
$\Delta\Delta E_{DIR}$	$+1.1\times10^{-8}$	$+1.1\times10^{-9}$	$+1.9\times10^{-9}$	-
$\Delta\Delta E_{TUR}$	$+1.3\times10^{-5}$	$+1.0\times10^{-6}$	$+3.6\times10^{-7}$	$+1.9\times10^{-6}$

The quadrature weights proposed by Becke were used in all calculations.[50] For calculations with the DIRAC and TURBOMOLE codes, the finest available grids were used, which are similar to the one chosen with our implementation. Calculations were performed with the SVWN5 LDA functional,[51,52] The PBE GGA functional,[53] and the PBE0 hybrid-GGA functional.[54]

IV. RESULTS AND DISCUSSION

We discuss below several aspects of the methodologies formally illustrated in Section II: i) we compare our implementation to those available in other codes; ii) we document the reduction to the collinear limit of different non-collinear formulations of the DFT; iii) we quantify the degree of rotational invariance of different non-collinear formulations; iv) we explicitly investigate the effect of the starting guess magnetization on the convergence of the SCF and on the obtained electronic solution for the various formulations.

A. Comparison with Previous Implementations

We first report comparisons of our implementation with those available in the DIRAC and TURBOMOLE codes, for validation purposes. We start by discussing re-

sults on the closed-shell electronic configurations, where since the magnetization is vanishingly small, all of the formulations coincide. Energies were converged down to 1×10^{-9} Ha for all implementations, and calculations were performed with and without the SOC operator included in the Hamiltonian, and the energy differences of these two calculations, ΔE_{SOC}, are tabulated.

In Table I, we report the ΔE_{SOC} calculated with our implementation, as well as the differences of the ΔE_{SOC} with respect to those calculated with the other implementations. These are denoted in the table as $\Delta\Delta E_X$, where X denotes the code used for the calculation, that is X = TUR or DIR. It can be seen from the table that the agreement with DIRAC is very satisfactory in all cases, because the $\Delta\Delta E_{DIR}$ is always on the order of 1×10^{-9} Ha, which is remarkably the same accuracy as the convergence of the SCF. The only exception is the PBE or PBE0 calculations on I_2, where the $\Delta\Delta E_{DIR}$ is instead on the order of 1×10^{-8} Ha.

As was also noted in Part I,[31] for the case of TlBr, it was not possible to use the DIRAC code in exactly the same computational conditions as in the other codes. This is due to the fact that the RECP-SOC implementation in DIRAC is only available with a basis of Cartesian Gaussian-type functions that differ from spherical Gaussian-type functions (used in our implementation as well as in the TURBOMOLE one) starting from angular momentum $l = 2$ (i.e. starting from d-type functions). Given that TlBr has occupied d orbitals in the valence, it was not possible to perform the comparison with DIRAC in this case. For all other molecular systems, no $l = 2$ or higher angular momentum functions were included in the valence basis sets, so that we were able to perform the comparison.

The agreement with TURBOMOLE is still very satisfactory but less good because this implementation uses the resolution of identity (RI) approximation for at least the evaluation of the Coulomb integrals. The RI approximation introduces inaccuracies which do not perfectly cancel between the calculations with and without SOC. As such, the $\Delta\Delta E_{TUR}$ are on the order of 1×10^{-5} Ha (for the I_2 molecule) to 1×10^{-7} Ha (for the IH molecule). These values are however still more than sufficient to confirm the correctness of the implementation, being two to four orders of magnitude smaller than the SOC contribution to the energy. The agreement with both codes is generally better with LDA (where only the density needs to be evaluated on the numerical grid), or with PBE0 (which includes a significant portion of Fock exchange, and hence is in a larger part analytical). A worst agreement is generally found using PBE, where both the density and its gradient need to be evaluated on the numerical grid.

We now discuss the calculations on the open-shell electronic configurations, which are obtained by removing one electron from the same molecules discussed above. As in Part I, we were unable to perform comparable calculations with the DIRAC code on open-shell electronic configurations as, to the best of our knowledge, it is not possible to perform single-determinant Kramers-unrestricted calculations with the DIRAC code at present. So the comparison can only be made against the TURBOMOLE code. What is more, we are only able to use one formulation for each functional, using the TURBOMOLE code. That is, the canonical non-collinear formulation for the LDA and the collinear formulation for the GGA. The comparison of calculations done using these formulations with both implementations is reported in Table II. It can be seen from Tables I and II that the SOC contribution to the total energy, ΔE_{SOC}, is now increased by a factor of three to four by removing one electron from all systems, except for TlBr, where the ΔE_{SOC} instead only increases by about 10%. A similar result was reported in Part I with the HF theory. The comparison with the TURBOMOLE implementation is now slightly less impressive than for the closed-shell systems, because the evaluation of the xc matrix elements and potential now also requires a numerical integration containing functions of the magnetization (and possibly its gradient) and not only the density. The $\Delta\Delta E_{TUR}$ is now mostly on the order of 1×10^{-4} Ha, except for $TlBr^+$, where it is instead on the order of 1×10^{-3} Ha. We note, however that the $\Delta\Delta E_{TUR}$ is still at least one order of magnitude smaller (in absolute value) than the ΔE_{SOC}, which helps confirm the correctness of the implementations.

TABLE II. Energies for the open-shell electronic configurations. See caption of Table I for a definition of all quantities. Values are given in atomic units (Ha). Calculations are performed with the canonical non-collinear theory for LDA and the collinear theory for PBE and PBE0.

	I_2^+	CH_3I^+	IH^+	$TlBr^+$
LDA				
ΔE_{SOC}	-2.2×10^{-2}	-1.6×10^{-2}	-1.6×10^{-2}	-4.2×10^{-2}
$\Delta\Delta E_{TUR}$	$+8.9\times10^{-5}$	$+1.6\times10^{-4}$	$+1.3\times10^{-4}$	$+4.1\times10^{-3}$
PBE				
ΔE_{SOC}	-2.1×10^{-2}	-1.4×10^{-2}	-1.4×10^{-2}	-3.9×10^{-2}
$\Delta\Delta E_{TUR}$	$+9.8\times10^{-5}$	$+1.7\times10^{-4}$	$+1.5\times10^{-4}$	$+1.3\times10^{-3}$
PBE0				
ΔE_{SOC}	-2.1×10^{-2}	-1.4×10^{-2}	-1.4×10^{-2}	-3.9×10^{-2}
$\Delta\Delta E_{TUR}$	$+1.1\times10^{-4}$	$+1.8\times10^{-4}$	$+1.5\times10^{-4}$	$+2.1\times10^{-3}$

B. The Reduction to the Collinear Limit of Non-Collinear Theories

We discuss now the reduction to the collinear limit of non-collinear formulations of the DFT, that is the ability of non-collinear theories to provide the same energy of

TABLE III. Deviation from the collinear limit of various non-collinear formulations (C stands for "canonical", SF for "Scalmani-Frisch", SC for our "signed canonical"). The reported quantities are energy differences (in atomic units) between non-collinear formulations and the collinear one for the open-shell electronic configurations in the absence of SOC. The "n.c." indicates that we were unable to converge the CH_3I^+ case to the desired energy tolerance using the canonical non-collinear formulation with PBE and PBE0.

	I_2^+	CH_3I^+	IH^+	$TlBr^+$
LDA				
C	$<10^{-15}$	-1.00×10^{-12}	$<10^{-15}$	$<10^{-15}$
PBE				
C	-1.28×10^{-2}	n.c.	-4.31×10^{-2}	-5.90×10^{-4}
SF	-1.16×10^{-2}	-2.82×10^{-2}	-3.42×10^{-2}	-5.80×10^{-4}
SC	-1.61×10^{-8}	-1.37×10^{-7}	-4.87×10^{-8}	$+1.00\times10^{-8}$
PBE0				
C	-1.03×10^{-2}	n.c.	-2.81×10^{-2}	-6.47×10^{-4}
SF	-8.56×10^{-3}	-1.92×10^{-2}	-2.18×10^{-2}	-6.00×10^{-4}
SC	-2.62×10^{-8}	-3.91×10^{-8}	-8.54×10^{-9}	-1.95×10^{-8}

the collinear theory in those cases where the magnetization is everywhere collinear. To do so, we consider the four open-shell systems where the molecules and guess magnetization are both oriented along z. The calculations are performed without SOC (i.e. in the absence of any torque that can rotate the initial magnetization) so that the magnetization remains aligned to z everywhere.

Table III reports the energy differences between the collinear theory and the different NC formulations (C stands for "canonical", SF for "Scalmani-Frisch", SC for our "signed canonical"). For the LDA, the three formulations coincide, but they differ for the GGA. The SCF for the more stable LDA and SC GGA formulations is converged down to 1×10^{-15} Ha, while it is only converged down to 1×10^{-8} Ha for the less stable C and SF GGA formulations. If a NC formulation reduces mathematically (and also numerically) to the collinear limit, then a vanishingly small energy difference should be found in the table. In fact, the table does show that this is the case for the NC formulation of the LDA, as the deviation from the collinear limit is always smaller than 1×10^{-15} Ha (in absolute value), with the only exception being the case of the CH_3I^+ molecule, where the energy difference is however still a vanishingly small value of -1×10^{-12} Ha.

More interestingly, it is also clear that both the C and SF formulations of GGA do not properly reduce to the collinear limit, with energy differences on the order of 1×10^{-4} to 1×10^{-2} Ha. In this respect, we note that the deviations are consistently slightly smaller for SF compared to C. The SF formulation is also slightly more numerically stable, as for example we were not able to converge the GGA calculations on the CH_3I^+ molecule using the C formulation while we were able to converge it using the SF formulation. In contrast to the previously reported formulations of non-collinear DFT, our "signed canonical" formulation is seen to properly reduce to the collinear limit, with deviations on the order of 1×10^{-7} to 1×10^{-9} Ha.

We now rationalize the failure of the C and SF non-collinear formulations to reach the same solution as the collinear theory in the collinear limit (i.e. when $m_x = m_y = 0$ everywhere). This failure originates from the inconsistencies in the sign of certain terms in the expressions for the xc magnetic field part of the potential $\underline{\boldsymbol{\mathcal{B}}}^{\boldsymbol{xc}}$, which reduces to $\underline{\boldsymbol{\mathcal{B}}}^{\boldsymbol{xc}} \rightarrow \mathcal{B}_z^{xc}$.

Before addressing the deficiencies of the GGA expressions, let us start by discussing the LDA case. In the collinear formulation for LDA, from Eqs. (21) and (26)-(29), the $\mathcal{B}_z^{xc}$ is a function of m_z (i.e. $\mathcal{B}_z^{xc}[m_z]$) and each term in the xc magnetic field carries the sign of m_z. On the other hand, in the SF or C formulations, from Eq. (15) as well as Eqs. (35)-(41), the derivatives of the functionals contained in the xc magnetic field, in the collinear limit reduce from functions of m to functions of $|m_z|$, so that the information on the sign of m_z would be lost. However, the sign is regained from the m_c/m pre-factors in Eq. (43), which reduce according to $m_c/m \rightarrow \mathrm{sgn}(m_z)$, such that the final expression for the xc potential is equivalent in all three formulations, for the LDA.

Now for the case of GGA, we first note that, within the collinear formulation, considering also Eqs. (31) and (32), the xc magnetic field is now a function of m_z and $|\underline{\boldsymbol{\nabla}} m_z|^2$ (i.e. $\mathcal{B}_z^{xc} = \mathcal{B}_z^{xc}[m_z, |\underline{\boldsymbol{\nabla}} m_z|^2]$) and each term in the xc magnetic field either carries the sign of m_z or is positive. On the other hand, in the SF or C formulations, from Eqs. (47), (50) and (53)-(57), the derivatives of the functionals contained in the xc magnetic field are functions of m and $|\underline{\boldsymbol{\nabla}} m|^2$ (for C) or functions of m and other gradient variables like, for example, $\underline{\boldsymbol{\nabla}}\ \underline{\mathbf{m}} \cdot \circ \underline{\boldsymbol{\nabla}}\ \underline{\mathbf{m}}$ (for SF). In both cases (C and SF), in the collinear limit, all of the variables reduce to $|m_z|$ and $|\underline{\boldsymbol{\nabla}} m_z|^2$, and some terms are multiplied by the pre-factors m_z/m in the expression for the xc magnetic field, see Eqs. (52) and (57), such that now the gradient terms have the wrong sign, when compared to the collinear formulation. As a result of this inconsistency of signs, the C and SF formulations yield erroneous solutions in the collinear limit. To be more precise, while all terms are multiplied by the pre-factors m_z/m in the C formulation, only those terms of the potential containing the functional derivatives with respect to n_+ and n_- are multiplied by the pre-factors m_z/m in the SF formulation, which explains why the SF formulation is slightly closer to the collinear limit than the C one.

TABLE IV. Rotational invariance of GGA collinear and non-collinear formulations of DFT with SOC. The linear I_2^+ molecule is studied in seven different orientations (from parallel to the z axis, 0°, to the x axis, 90°). The atomic guess magnetization is always parallel to the axis of the molecule. For all calculations, the SCF is converged down to 1×10^{-8} Ha. For each orientation, the absolute difference (in Ha) between the computed energy and that obtained when the molecule is along z ($|E-E_z|$), and the number of cycles needed to converge the SCF are reported. The last row reports the average over all the explored orientations, |av|, of the absolute value of the quantities in their respective columns.

	Collinear				Non-Collinear											
					Canonical				Scalmani-Frisch				Signed Canonical			
	PBE		PBE0		PBE		PBE0		PBE		PBE0		PBE		PBE0	
0°	Ref.	27	Ref.	34	Ref.	94	Ref.	100	Ref.	94	Ref.	105	Ref.	23	Ref.	34
10°	7.7×10^{-5}	27	6.3×10^{-5}	41	4.5×10^{-4}	95	4.0×10^{-4}	109	6.4×10^{-3}	589	3.5×10^{-4}	125	1.0×10^{-5}	29	1.1×10^{-6}	35
22°	3.9×10^{-4}	27	3.1×10^{-4}	54	1.1×10^{-3}	130	9.4×10^{-4}	123	8.5×10^{-3}	402	8.5×10^{-4}	136	9.6×10^{-6}	26	1.3×10^{-6}	33
45°	1.5×10^{-3}	28	1.2×10^{-3}	74	1.4×10^{-3}	99	1.1×10^{-3}	100	1.5×10^{-3}	99	1.1×10^{-3}	67	9.7×10^{-6}	29	4.8×10^{-7}	32
68°	1.9×10^{-3}	166	2.4×10^{-3}	101	1.2×10^{-3}	89	1.0×10^{-3}	129	9.0×10^{-3}	407	9.3×10^{-4}	100	7.8×10^{-6}	26	2.0×10^{-7}	35
80°	1.7×10^{-3}	90	3.0×10^{-3}	116	6.2×10^{-4}	101	5.4×10^{-4}	100	6.9×10^{-3}	694	4.9×10^{-4}	170	1.4×10^{-5}	27	1.1×10^{-6}	31
90°	1.6×10^{-3}	27	3.2×10^{-3}	32	2.2×10^{-4}	91	1.8×10^{-4}	97	2.3×10^{-4}	93	1.7×10^{-4}	104	1.8×10^{-6}	24	1.4×10^{-6}	35
|av|	1.2×10^{-3}	56	1.7×10^{-3}	65	8.4×10^{-4}	100	7.0×10^{-4}	108	5.4×10^{-3}	340	6.5×10^{-4}	115	8.9×10^{-6}	26	9.3×10^{-7}	34

In contrast, in our SC formulation, the correct sign (when compared with the corresponding expressions from the collinear formulation) is included from the start in the expressions for the variables on which the xc functional (and potential) depends and therefore the correct collinear limit can be achieved. We remind the reader that this analysis is independent on the specific form of the GGA functional and therefore formally holds for all GGA functionals. Finally, we stress that, even with our SC non-collinear formulation, the reduction to the collinear limit for GGA is not quite as good as for LDA. This is essentially because of the need for the screening procedure described in Section II D 4, which does introduce a certain amount of numerical noise.

C. The Rotational Invariance of Non-Collinear Theories

We now discuss the rotational invariance of the collinear approach and of the various non-collinear formulations, in the presence of SOC. The tests are performed on the I_2^+ linear molecule, for which seven different orientations are explored: from parallel to the z axis, 0°, to parallel to the x axis, 90°. At each orientation, an initial atomic guess for the magnetization is used, which is parallel to the molecular axis. For all calculations, the SCF is converged down to 1×10^{-8} Ha. The absolute differences between the energies of the various orientations with respect to that obtained when the molecule is along z (taken as a reference) are reported in Table IV for the plain GGA functional PBE and hybrid GGA functional PBE0, or Table V for the LDA functional. In the ESI, we provide additional data using instead the BLYP GGA functional, which however yields similar results.[55,56] The last row of both tables reports average energy differences over all the explored orientations. For perfectly rotationally invariant formulations of the theory the reported energy differences should be vanishingly small. Any significant deviation from small values indicates either that the formulation is formally not rotationally invariant, or that it is excessively polluted by numerical noise in the calculation procedure.

From Tables IV and V, it is clear that, as expected, the collinear approach does not ensure rotational invariance when the SOC operator is included in the Hamiltonian, both at LDA and GGA level. Indeed, the average deviation of the energy among different orientations is very large, on the order of 1×10^{-3} Ha for LDA, PBE and PBE0. For the case of LDA, the rotational invariance is fully regained by the non-collinear formulation, as the average deviation becomes 1.7×10^{-8} Ha. It is interesting to note that this is exactly the same value obtained for the collinear formulation without SOC, thus indicating that our implementation of non-collinear LDA is as numerically accurate as the previously existing one-component collinear code.

On the other hand, for GGA xc functionals, the various non-collinear formulations show different behaviors with regards to their rotational invariance. In particular, from Table IV, it is seen that both the C and SF

TABLE V. Same as Table IV, but now results are reported for the LDA, using both the collinear or non-collinear theories, with and without the inclusion of the SOC operator in the Hamiltonian.

	Collinear				Non-Collinear			
	with SOC		without SOC		with SOC		without SOC	
0°	Ref.	25	Ref.	27	Ref.	25	Ref.	27
10°	7.1×10^{-5}	25	7.1×10^{-9}	27	8.9×10^{-9}	25	7.1×10^{-9}	27
22°	3.6×10^{-4}	25	1.2×10^{-8}	27	1.0×10^{-8}	25	1.2×10^{-8}	27
45°	1.4×10^{-3}	27	6.4×10^{-8}	27	6.5×10^{-8}	25	6.5×10^{-8}	27
68°	2.8×10^{-3}	35	1.1×10^{-8}	27	1.1×10^{-8}	25	1.2×10^{-8}	27
80°	1.9×10^{-3}	95	8.8×10^{-9}	27	8.9×10^{-9}	25	7.1×10^{-9}	27
90°	1.9×10^{-3}	25	2.0×10^{-9}	27	2.8×10^{-10}	25	2.1×10^{-10}	27
|av|	1.4×10^{-3}	37	1.7×10^{-8}	27	1.7×10^{-8}	25	1.7×10^{-8}	27

formulations clearly do not ensure rotational invariance, and in fact only marginally improve with respect to a purely collinear description, in this context (with average energy deviations among different orientations on the order of 5×10^{-3} to 8×10^{-4} Ha). In particular, with PBE and the SF formulation, the average deviation, 5.4×10^{-3} Ha, is actually worse than from the collinear formulation, 1.2×10^{-3} Ha.

At variance with the previously suggested C and SF formulations of non-collinear GGA, our "signed canonical" theory does ensure the desired rotational invariance, as now the average energy deviation is on the order of 9×10^{-6} to 9×10^{-7} Ha. The reason for the failure of the C and SF formulations to achieve rotational invariance is two-fold. First, following the logic above giving formal arguments for their failure to reach the collinear limit, we expect that, on a given point in the DFT grid, certain terms of the xc potential will carry the wrong sign, depending on the local sign of the Cartesian components of the magnetization and their derivatives. As the molecule is rotated in the Cartesian frame, a greater or lesser number of points in the DFT grid can have associated terms in the xc potential that carry the wrong sign, such that the calculated energy is no longer rotationally invariant. The second reason is that they depend more heavily on the screening described in Section II D 4, given that they are less numerically stable, and this of course introduces numerical noise.

The higher numerical stability of our SC formulation compared to the C and SF ones is also reflected in the number of cycles needed to converge the SCF within the same energy threshold of 1×10^{-8} Ha. These numbers are also reported for each calculation in Tables IV and V. For PBE calculations, our SC theory requires 26 cycles to converge the SCF on average while the C formulation takes 100 cycles and the SF one 340 cycles. For PBE0 calculations, 34 iterations are needed with our SC theory while 108 and 115 are required by the C and SF formulations, respectively.

Table IV also allows to investigate the effect of the inclusion into the xc functional of a fraction of Fock exchange, as in the hybrid PBE0 functional. While we discuss from a formal point of view the connection between Fock exchange and the orbital current-density within a two-component non-collinear formalism in a another publication,[37] here we note that the inclusion of Fock exchange systematically improves the rotational invariance by about one order of magnitude for both the SF and SC theories.

At the same time, the inclusion of Fock exchange almost always increases the amount of cycles needed to converge the SCF. The exception is with the SF formulation, where as will be discussed below, with PBE and for certain orientations (namely 10°, 22°, 68° and 80° from the z axis), the SCF falls into a qualitatively different solution and this increases the amount of needed SCF cycles. In this particular case, the inclusion of Fock exchange also helps retrieve rotational invariance of the energy (as the reported differences for PBE0 are smaller than for PBE), regain a qualitatively similar solution as obtained with the other orientations, but also (unlike in the other cases) reduce the amount of needed SCF cycles.

So far, we have discussed the rotational invariance of the different non-collinear GGA theories by looking at the energy of different orientations. We now analyze the spatial distribution of the magnetization as well. Figure 1 shows 2D maps of the computed magnetization of the I_2^+ molecule in the xz plane as the molecule is rotated from x (left panels) to z (right panels) for the C, SF and SC formulations, with the PBE functional. At each orientation, the initial atomic guess is consistently parallel to the molecular axis. The small black arrows in the figure have lengths which reflect the magnitude and direction of the x and z components of the magnetization, while the color represents the magnitude m of the magnetization vector. The absolute value of the energy difference of each solution with respect to that obtained with the molecule along z is reported on top of the panels, as well as the number of cycles needed to converge the SCF, on the bottom of the panels.

Given that consistent conditions are used for each calculation as the system is rotated, a satisfactory non-collinear GGA formulation should yield at least a qualitatively similar distribution of magnetization in all cases. It

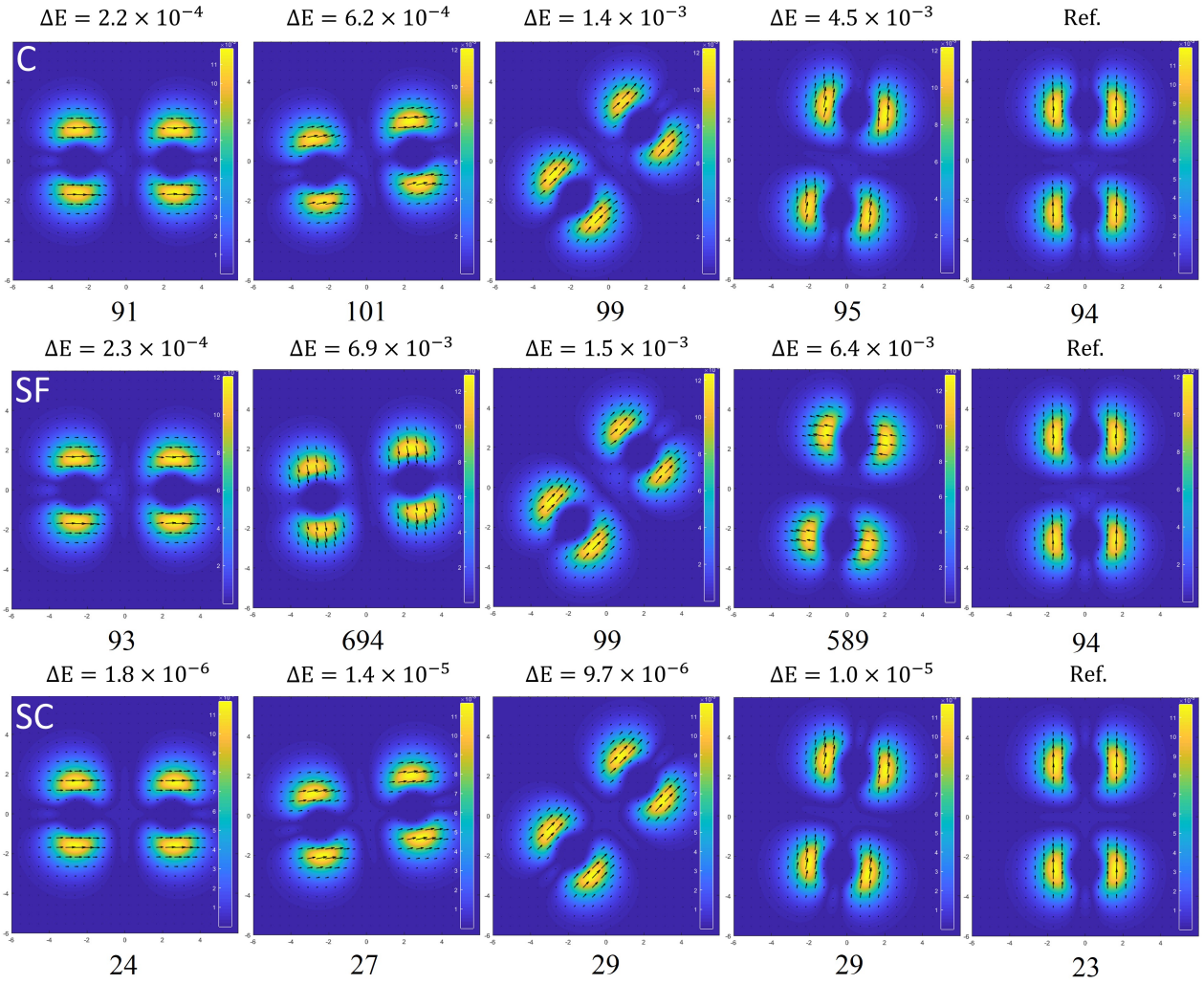

FIG. 1. Spatial distribution of the electronic magnetization for the I_2^+ molecule in the xz plane, as computed with the PBE xc functional, upon inclusion of SOC, with three formulations of the non-collinear GGA theory: canonical C, Scalmani-Frisch SF, and "signed canonical" SC. The molecular axis and atomic guess magnetization is progressively rotated from the x axis (left) to the z axis (right). The small black arrows in the figure have lengths which reflect the magnitude and direction of the x and z components of the magnetization, while the color represents the magnitude m of the magnetization vector. The absolute value of the energy difference of each solution with respect to that obtained with the molecule along z is reported on top of the panels, as well as the number of cycles needed to converge the SCF, on the bottom of the panels. All quantities are reported in atomic units.

can be seen from the figure that the C formulation, while not providing a quantitatively invariant description (see discussion on the energy above), provides electronic solutions that are qualitatively similar for each plotted orientation, with the magnetization being almost parallel to the axis of the molecule everywhere. On the contrary, the SF formulation yields even qualitatively different solutions for two (second and fourth from the left) of the five plotted orientations, with the magnetization pointing perpendicular to the axis of the molecule in these cases.

The only formulation of non-collinear GGA that is found to ensure both a quantitative rotational invariance (from the point of view of the calculated energies) and a qualitative rotational invariance (by looking at the plot of the magnetization) is our "signed canonical" formulation.

D. The Effect of the Initial Guess

We discuss the effect of the initial guess on the obtained electronic solution and convergence of the SCF procedure for the different formulations of non-collinear DFT in the presence of a SOC operator.

We start by discussing the effect of different guesses for the density matrix on LDA non-collinear calculations. We consider different non-collinear guesses with the same orientation of the guess magnetization on both centers of

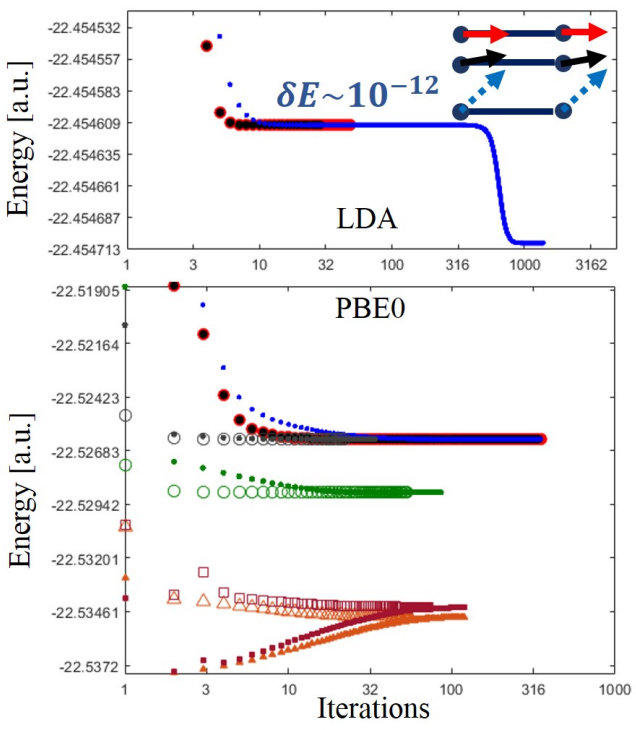

FIG. 2. The evolution of the energy during the SCF is shown for the I_2^+ molecule as obtained with different non-collinear formulations using the LDA (top panel) or a GGA xc functional (bottom panel). Top panel: three different atomic guesses are used, whose atomic magnetization is schematically represented in the inset. The color of the curves matches that of the arrows defining the initial magnetization. Bottom panel: non-collinear PBE0 calculations. For the SC formulation, the same three atomic guesses are used (same colors and symbols of top panel), along with guesses from density matrices of previous GHF (filled circles) and non-collinear LDA (open circles) calculations for the meta-stable (grey) and most stable (green) electronic configurations. Similarly, the maroon open and filled squares are calculations starting from the LDA or GHF most stable solutions but now with the C formulation; the orange open and filled triangles are calculations starting from the LDA or GHF most stable solutions with the SF formulation.

the molecule. The SCF is converged down to 1×10^{-15} Ha. The top panel of Figure 2 shows SCF energy profiles for the I_2^+ molecule, as obtained by starting from different atomic guesses for the magnetization, imposed based on the strategy outlined in Part I.[31] Three different atomic guesses are used, whose atomic magnetization is schematically represented on the top right corner of the figure, with the same notation used in Part I (i.e. the direction of the colored arrows show the orientation of the guess magnetization on each atomic center). The three colored curves are SCF energy profiles obtained using the three atomic guesses of the same color: the black guess is parallel to the axis of the molecule (z direction), the red guess is one degree off of the axis of the molecule, and the blue guess is along the xyz diagonal. The values are reported on a log-log scale.

Analogously to what already observed from GHF calculations in Part I, also in this case, different atomic guesses lead to different obtained solutions. It is seen from the figure that the SCF reaches convergence at a metastable solution (referred to in the following as the LDA metastable solution) using both the red and black guesses, while it reaches another solution (referred to in the following as the LDA most stable solution) that is 9.87×10^{-5} Ha lower in energy using the blue guess. We note that the blue curve goes through a plateau (i.e. a region of relatively flat energy variation), whereby the energy difference between two successive cycles is as low as 1×10^{-12} Ha, as denoted with the δE on the figure. The need to overcome such small energy variations in order to reach the most stable electronic configuration makes the numerical stability of the code of primary importance, as was also the case for the HF theory in Part I.[31] Luckily, non-collinear LDA is a well-defined theory, which ensures the required numerical stability.

Now, let us analyze the non-collinear GGA results, obtained with the PBE0 xc functional: SCF energy profiles are reported in the lower panel of Figure 2. The same three atomic guesses discussed above for LDA are also used here with the various non-collinear formulations. Results are shown only for the SC theory (blue, red and black circles in the lower panel of the figure) as the other formulations yield similar results. It is evident that, in this case, no atomic guess is able to drive the SCF towards the most stable solution, and the metastable solution is always found. This is because, unlike LDA, the more numerically sensitive GGA formulations are unable to overcome the challenging plateau with energy variations as small as 1×10^{-12} Ha. This is a very critical limitation of non-collinear GGA formulations, which, however, we were able to overcome. Indeed, by starting the SCF with a previously calculated non-collinear LDA (open symbols) or GHF (filled symbols) density matrix corresponding to the most stable solution, we were able to converge any non-collinear GGA formulation to the right solution (C in maroon, SF in orange and SC in green; the energy varies because different formulations correspond to different xc potentials).

This highlights the usefulness of using a previously calculated density matrix from a numerically more robust theory, like non-collinear LDA or GHF before doing more challenging GGA calculations. This is indeed the computational strategy that we recommend when one wants to possibly reach the true most stable electronic configuration.

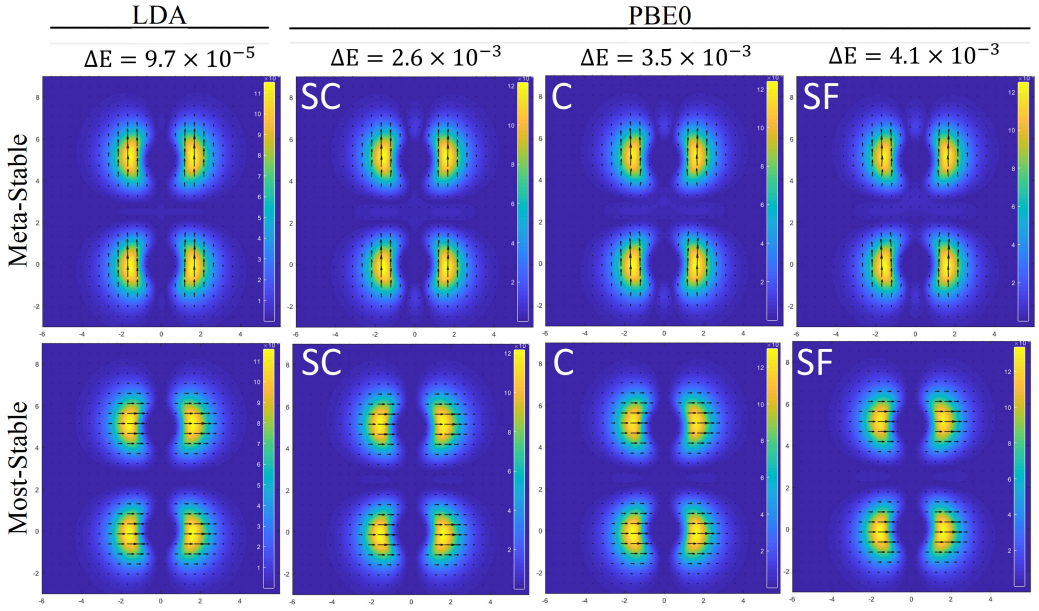

FIG. 3. Spatial distribution of the electronic magnetization for the I_2^+ molecule in the xz plane, as obtained for the meta-stable electronic configuration (top panels) and the most stable electronic configuration (bottom panels) with the non-collinear LDA and with the three different formulations of non-collinear PBE0. For PBE0 calculations, the corresponding LDA solution is used as a starting guess. The ΔE reported on the top of the panels is the energy difference between the meta-stable and most stable electronic configurations. The graphical representation is analogous to that of Figure 1.

We further note that for all of the formulations, the GGA calculations converge in less cycles by using an LDA starting guess rather than a GHF one. It can also be seen that our SC formulation converges in much less cycles and in a more regular way than the C and SF formulations (compare green curves for SC versus maroon and orange curves for C and SF). What is more, with both previously reported theories (C and SF), by starting from a GHF guess, the SCF has an un-satisfactory behavior, whereby the energy surpasses the global minimum and increases in value (see maroon and orange filled shapes at the bottom of the panel). Given that this behavior is noticed in the canonical but not in our "signed canonical" theory, and given that the only difference between these two formulations is the assignment of the sign of the magnetization in the xc potential, we conclude that this non-variational increase in energy must be the result of improper assignment of the sign in the xc potential for the C and SF theories.

Finally, we want to analyze the obtained solutions in terms of the spatial distribution of the magnetization. Figure 3 reports 2D maps of the magnetization in the xz plane, with the same graphical representation already introduced for Figure 1. We see that, analogously to what already observed from GHF calculations in Part I, the metastable electronic configuration is characterized by a magnetization that is everywhere parallel to the molecular axis while the most stable configuration has a magnetization perpendicular to the molecular axis. Non-collinear PBE0 calculations are performed by starting the SCF from the corresponding LDA solutions as an initial guess. We observe that the computational strategy introduced before (i.e. by starting non-collinear GGA calculations from the solution of a previous non-collinear LDA or GHF solution) ensures to get the same electronic solution (i.e. with the same qualitative distribution of the magnetization) regardless of the xc functional or formulation used, which is rather satisfactory.

V. CONCLUSIONS

The formalism of Kramers-unrestricted collinear and all previously reported formulations of non-collinear density functional theory (DFT) for the self-consistent treatment of spin-orbit coupling (SOC) in electronic structure calculations has been revised. The various approaches have been implemented in the CRYSTAL program and have been compared both formally and using test examples on small molecules.

While the existing approaches are satisfactory for use with the local density approximation (LDA), the numerical tests and formal analysis have allowed us to highlight several deficiencies for their extension to the generalized gradient approximation (GGA). These include: i) the failure of non-collinear theories to reduce to the proper collinear limit; ii) the failure to ensure a quantitative rotational invariance of the total energy when a SOC operator is included in the Hamiltonian; iii) the failure to provide a qualitative rotational invariance of the

spatial distribution of the magnetization when a SOC operator is included in the Hamiltonian; iv) a possible non-variational behavior of the energy along the self-consistent field process.

All of the above mentioned problems are shown (both formally and through test examples) to be solved by using instead a new formulation of non-collinear DFT for GGA functionals, which we call the "signed canonical" theory.

The effect of the starting guess density matrix on the obtained solution is discussed for the various non-collinear theories. More specifically, we show the benefits of using a GHF or non-collinear LDA solution as a starting guess for subsequent non-collinear GGA calculations, as this allows to surpass difficult obstacles in the rugged energy landscape.

SUPPLEMENTARY MATERIAL

See supplementary material for a table showing the degree of rotational invariance of our signed canonical formulation when the BLYP functional is used.

ACKNOWLEDGEMENTS

J.K.D. is grateful to the National Science and Engineering Research Council of the Government of Canada for a Vanier scholarship.

[1] G. Vignale and M. Rasolt, Phys. Rev. B **37**, 10685 (1988).
[2] E. Engel, in *Theor. Comput. Chem.* (Elsevier, 2002), vol. 11, pp. 523–621.
[3] C. van Wüllen, in *Theor. Comput. Chem.* (Elsevier, 2004), vol. 14, pp. 598–655.
[4] J. Paquier and J. Toulouse, J. Chem. Phys. **149**, 174110 (2018).
[5] J. Kubler, K.-H. Hock, J. Sticht, and A. Williams, J. Phys. F **18**, 469 (1988).
[6] I. W. Bulik, G. Scalmani, M. J. Frisch, and G. E. Scuseria, Phys. Rev. B **87**, 035117 (2013).
[7] J. E. Peralta, G. E. Scuseria, and M. J. Frisch, Phys. Rev. B **75**, 125119 (2007).
[8] D. Hobbs, G. Kresse, and J. Hafner, Phys. Rev. B **62**, 11556 (2000).
[9] G. Scalmani and M. J. Frisch, J. Chem. Theor. Comput. **8**, 2193 (2012).
[10] K. Knöpfle, L. Sandratskii, and J. Kübler, Phys. Rev. B **62**, 5564 (2000).
[11] V. García-Suárez, C. Newman, C. J. Lambert, J. Pruneda, and J. Ferrer, Eur. Phys. J. B **40**, 371 (2004).
[12] P. Kurz, F. Förster, L. Nordström, G. Bihlmayer, and S. Blügel, Phys. Rev. B **69**, 024415 (2004).
[13] A. Dal Corso and A. M. Conte, Phys. Rev. B **71**, 115106 (2005).
[14] M. K. Armbruster, F. Weigend, C. van Wüllen, and W. Klopper, Phys. Chem. Chem. Phys. **10**, 1748 (2008).
[15] F. Egidi, S. Sun, J. J. Goings, G. Scalmani, M. J. Frisch, and X. Li, J. Chem. Theor. Comput. **13**, 2591 (2017).
[16] C. Van Wüllen, J. Comput. Chem. **23**, 779 (2002).
[17] E. Trushin and A. Görling, Phys. Rev. B **98**, 205137 (2018).
[18] S. Sharma, J. Dewhurst, C. Ambrosch-Draxl, S. Kurth, N. Helbig, S. Pittalis, S. Shallcross, L. Nordström, and E. Gross, Phys. Rev. Lett. **98**, 196405 (2007).
[19] V. Vallet, L. Maron, C. Teichteil, and J.-P. Flament, J. Chem. Phys. **113**, 1391 (2000).
[20] S. Yabushita, Z. Zhang, and R. M. Pitzer, J. Phys. Chem. A **103**, 5791 (1999).
[21] L. Visscher, K. G. Dyall, and T. J. Lee, Int. J. of Q. Chem. **56**, 411 (1995).
[22] W. Liu and Y. Xiao, Chem. Soc. Rev. **47**, 4481 (2018).
[23] F. Wang and T. Ziegler, J. Chem. Phys. **121**, 12191 (2004).
[24] F. Wang and T. Ziegler, J. Chem. Phys. **122**, 074109 (2005).
[25] M. Huix-Rotllant, B. Natarajan, A. Ipatov, C. M. Wawire, T. Deutsch, and M. E. Casida, PCCP **12**, 12811 (2010).
[26] Z. Rinkevicius and H. Ågren, Chem. Phys. Lett. **491**, 132 (2010).
[27] Z. Rinkevicius, O. Vahtras, and H. Ågren, J. Chem. Phys. **133**, 114104 (2010).
[28] Z. Li and W. Liu, J. Chem. Phys. **136**, 024107 (2012).
[29] ReSpect 5.1.0 (2019), relativistic spectroscopy DFT program of authors M. Repisky, S. Komorovsky, V. G. Malkin, O. L. Malkina, M. Kaupp, K. Ruud, with contributions from R. Bast, R. Di Remigio, U. Ekstrom, M. Kadek, S. Knecht, L. Konecny, E. Malkin, I. Malkin Ondik (see http://www.respectprogram.org).
[30] J. Anton, B. Fricke, and E. Engel, Phys. Rev. A **69**, 012505 (2004).
[31] J. K. Desmarais, J.-P. Flament, and A. Erba, J. Chem. Phys. (2019), accepted.
[32] R. Dovesi, A. Erba, R. Orlando, C. M. Zicovich-Wilson, B. Civalleri, L. Maschio, M. Rérat, S. Casassa, J. Baima, S. Salustro, et al., WIREs Comput. Mol. Sci. **8**, e1360 (2018).
[33] H. Stoll, B. Metz, and M. Dolg, J. Comput. Chem. **23**, 767 (2002).
[34] L. Maron and C. Teichteil, Chem. Phys. **237**, 105 (1998).
[35] J. K. Desmarais, A. Erba, and R. Dovesi, Theor. Chem. Acc. **137**, 28 (2018).
[36] Z. Zhang, Theor. Chem. Acc. **133**, 1588 (2014).
[37] J. K. Desmarais, J.-P. Flament, and A. Erba, J. Phys. Chem. Lett. **10**, 3580 (2019).
[38] U. von Barth and L. Hedin, J. Phys. C **5**, 1629 (1972).
[39] K. Capelle, G. Vignale, and B. Györffy, Phys. Rev. Lett. **87**, 206403 (2001).
[40] A. Petrone, D. B. Williams-Young, S. Sun, T. F. Stetina, and X. Li, Eur. Phys. J. B **91**, 169 (2018).
[41] J. A. Pople, P. M. Gill, and B. G. Johnson, Chem. Phys. Lett. **199**, 557 (1992).
[42] In the present implementation, the mean quantities $\langle m_c/m \rangle$ are calculated by averaging the m_c/m over the atomic basin to which the current point of the DFT grid belongs. The size of each atomic basin is determined using the same atomic radii that are used to calculate the DFT integration weights. These quantities are computed from the values of the magnetization of the previous iteration of the SCF (or of the starting guess at the first iteration). Other choices for the partitioning of space for calculating the averaged $\langle m_c/m \rangle$ quantities could be possible but we leave this to future work.
[43] DIRAC, a relativistic ab initio electronic structure program, Release DIRAC17 (2017), written by L. Visscher, H. J. Aa. Jensen, R. Bast, T. Saue, and others (see `http://www.diracprogram.org`).
[44] *TURBOMOLE V7.3 2018, a development of University of Karlsruhe and Forschungszentrum Karlsruhe GmbH, 1989-2007, TURBOMOLE GmbH, since 2007; available from* `http://www.turbomole.com`.
[45] M. Valiev, E. J. Bylaska, N. Govind, K. Kowalski, T. P. Straatsma, H. J. Van Dam, D. Wang, J. Nieplocha, E. Apra, T. L. Windus, et al., Comput. Phys. Comm. **181**, 1477 (2010).
[46] P. Hohenberg and W. Kohn, Phys. Rev. **136**, B864 (1964).
[47] M. D. Towler, A. Zupan, and M. Causà, Comput. Phys. Comm. **98**, 181 (1996).
[48] V. I. Lebedev, USSR Comput. Math. Math. Phys. **16**, 10 (1976).
[49] V. I. Lebedev, Siber. Math. J. **18**, 99 (1977).
[50] A. D. Becke, J. Chem. Phys. **88**, 1053 (1988).
[51] P. A. Dirac, in *Math. Proc. Camb. Philo. Soc.* (Cambridge University Press, 1930), vol. 26, pp. 376–385.

[52]S. H. Vosko, L. Wilk, and M. Nusair, Can. J. Phys. **58**, 1200 (1980).
[53]J. P. Perdew, K. Burke, and M. Ernzerhof, Phys. Rev. Lett. **77**, 3865 (1996).
[54]C. Adamo and V. Barone, J. Chem. Phys. **110**, 6158 (1999).
[55]C. Lee, W. Yang, and R. G. Parr, Physical review B **37**, 785 (1988).
[56]A. D. Becke, Physical review A **38**, 3098 (1988).